



Regional, multi-decadal analysis reveals that stream temperature increases faster than air temperature

Hanieh Seyedhashemi^{1,2}, Jean-Philippe Vidal¹, Jacob S. Diamond¹, Dominique Thiéry³, Céline Monteil⁴, Frédéric Hendrickx⁴, Anthony Maire⁴, and Florentina Moatar¹

¹INRAE, UR RiverLy, 5 rue de la Doua CS 20244, 69625 Villeurbanne, France

²EA 6293 GéoHydrosystèmes COntinentaux, Université François-Rabelais de Tours, Parc de Grandmont, 37200 Tours, France

³BRGM, Bureau de Recherches Géologiques et Minières, BP 6009 45060 Orléans Cedex 2, France

⁴EDF – Recherche et Développement, Laboratoire National d’Hydraulique et Environnement, Chatou, France

Correspondence: Hanieh Seyedhashemi (hanieh.seyedhashemi@inrae.fr)

Abstract.

Stream temperature appears to be increasing globally, but its rate remains poorly constrained due to a paucity of long-term data and difficulty in parsing effects of hydroclimate and landscape variability. Here, we address these issues using the physically-based thermal model T-NET (Temperature-NETwork) coupled with the EROS semi-distributed hydrological model to reconstruct past daily stream temperature and streamflow at the scale of the entire Loire River basin in France (10⁵ km² with 52278 reaches). Stream temperature increased for almost all reaches in all seasons (mean = +0.38 °C/decade) over the 1963–2019 period. Increases were greatest in spring and summer with a median increase of +0.38 °C (range=+0.11– +0.76 °C) and +0.44 °C (+0.08– +1.02 °C) per decade, respectively. Rates of stream temperature increases were greater than for air temperature across seasons for 50–86 % of reaches. Spring and summer increases were typically the greatest in the southern headwaters (up to +1 °C/decade) and in the largest rivers (Strahler order >5). Importantly, air temperature and streamflow exerted joint influence on stream temperature trends, where the greatest stream temperature increases were accompanied by similar trends in air temperature (up to +0.71 °C/decade) and the greatest decreases in streamflow (up to -16 %/decade). Indeed, for the majority of reaches, positive stream temperature anomalies exhibited synchrony with positive anomalies in air temperature and negative anomalies in streamflow, highlighting the dual control exerted by these hydroclimatic drivers. Moreover, spring and summer stream temperature, air temperature, and streamflow time series exhibited common change-points occurring in the late 1980s, suggesting a temporal coherence between changes in the hydroclimatic drivers and a rapid stream temperature response. Critically, riparian vegetation shading mitigated stream temperature increases by up to 16 % in smaller streams (i.e., <30 km from the source). Our results provide strong support for basin-wide increases in stream temperature due to joint effects of rising air temperature and reduced streamflow. We suggest that some of these climate change-induced effects can be mitigated through the restoration and maintenance of riparian forests, and call for continued high-resolution monitoring of stream temperature at large scales.



1 Introduction

Stream temperature is a critical water quality parameter affecting the distribution of aquatic communities (Poole and Berman, 2001; Ducharne, 2008), but its future under global change remains uncertain. As air temperature (T_a) increases worldwide
25 due to climate change, stream temperature (T_w) is expected to follow a similar trajectory (Mohseni et al., 1999; Kaushal
et al., 2010; Van Vliet et al., 2011; Isaak et al., 2012; Arora et al., 2016). Indeed, there is growing evidence that stream
warming is occurring around the world, affecting freshwater ecosystems through structural and functional changes in biological
communities throughout the food web (Woodward et al., 2010; O’Gorman et al., 2012; Scheffers et al., 2016). Deleterious
warming effects are documented from bottom-dwelling microorganisms (e.g Romaní et al., 2016; Majdi et al., 2020) up to
30 macroinvertebrates (e.g Flourey et al., 2013; Bruno et al., 2019) and fish communities (e.g Maire et al., 2019; Stefani et al.,
2020). However, the paucity of long-term time series of T_w (Webb and Walling, 1996; Nelson and Palmer, 2007; Webb et al.,
2008; Arora et al., 2016) has impaired the larger scale assessment of such trends, especially in light of confounding factors
like hydrological changes and land use change. Hence, analyses of T_w trends, especially at large spatiotemporal scales, remain
scarce (but see Kaushal et al., 2010; Orr et al., 2015; Arora et al., 2016; Michel et al., 2020; Wilby and Johnson, 2020).

35 To overcome the lack of T_w data, large-scale ecological studies typically use T_a as a proxy for T_w to assess the impact of
climate change on the spatial distribution of aquatic organisms (e.g Buisson et al., 2008; Buisson and Grenouillet, 2009; Tisseuil
et al., 2012; Domisch et al., 2013), but T_a can be an imprecise surrogate for T_w (Caissie, 2006). Indeed, many landscape and
basin characteristics (e.g., stream discharge [Q], streambed morphology, karst resurgences, topography, and vegetation cover)
contribute to the response of T_w to climate change over time and space (Stefan and Preud’homme, 1993; Webb and Walling,
40 1996; Webb et al., 2008; Hannah and Garner, 2015). For instance, riparian vegetation can obstruct solar radiation, which is the
dominant heat flux at air-water surface (Caissie, 2006; Hannah et al., 2004), and therefore decrease T_w response to T_a (Loicq
et al., 2018; Johnson, 2004). However, while riparian vegetation shading can greatly decrease the temperature of small rivers
(Dan Moore et al., 2005; Loicq et al., 2018), it has limited effects on larger rivers since the width of such rivers is large enough
that only a small part of it can be shaded. Rising groundwater temperature (Taylor and Stefan, 2009; Kurylyk et al., 2013, 2014)
45 and reduced groundwater flows (Kurylyk et al., 2014) due to climate change may further contribute to T_w trends (Meisner,
1990; Arora et al., 2016), leading to asymmetric controls (vis-à-vis T_a) on T_w (Moatar and Gailhard, 2006), especially in
headwaters (Caissie, 2006; Kelleher et al., 2012; Mayer, 2012). Finally, intensification of the water cycle (Huntington, 2006),
with more frequent and severe droughts (Mantua et al., 2010; Giuntoli et al., 2013; Prudhomme et al., 2014), as well as more
intense and sudden floods (Blöschl et al., 2019) may decouple T_a - T_w trends, exacerbating T_w increases that will most likely
50 be evident during low summer flows when thermal capacity and flow velocity are at their minima (Webb, 1996; Webb et al.,
2008).

There is thus a clear need to improve our estimates of T_w trends to assess how stream ecosystems will respond in the face of
a changing climate. Unfortunately, extrapolating trend estimates derived from short time series may lead to paradoxical results,
e.g., cooling streams in a warming world (Arismendi et al., 2012). This discrepancy in short- and long-term dynamics is likely
55 due to confounding influences of T_a and hydrology, with implications for the persistence of specialized aquatic organisms (e.g.,



for cold-water biota, Arismendi et al., 2013b) and the completion of their life cycle (e.g., for diadromous fish, Arevalo et al., 2020). Hence from an ecological perspective, it will be critical to understand and deconvolve the joint influences of changing Tw and Q regimes. In the absence of more robust data sources, modeling is thus an indispensable tool in meeting these goals.

60 Tw models output data sets that can then be used to assess the magnitude of long-term trends, but model selection entails important considerations. For example, Tw can be estimated by developing a statistical, or stochastic, model based on multiple independent drivers (Benyahya et al., 2007), which is a common practice for large scale studies (e.g Mantua et al., 2010; Jackson et al., 2017, 2018). However, these statistical models lack mechanism; they cannot reveal the specific energy transfer mechanisms responsible for the spatiotemporal patterns of Tw (Dugdale et al., 2017). They are also unable to predict Tw
65 for periods other than those used for their calibration due to, for instance, the non-stationary relationship between Ta and Tw over time (Arismendi et al., 2014). Alternatively, physically-based, or deterministic, models are entirely mechanistic; they predict Tw dynamics through a heat budget, accounting for energy exchanges and effects of landscape characteristics on energy transfer (Sinokrot et al., 1995; Webb and Walling, 1997; Yearsley, 2009; van Vliet et al., 2013). Critically, such process-based models can be used not only to reconstruct past time series, but they can be used in forecasting, or in predicting Tw response
70 to projected climate or land-use changes (Dugdale et al., 2017; Caissie et al., 2007).

Here, we used a physical process-based thermal model coupled with a semi-distributed hydrological model to understand how Tw has responded to recent climate change at a large scale. To do so, we first assessed the performance of the models against field observations over the Loire basin, France, then reconstructed daily Q and Tw over the past 57 years over the whole hydrographic network. We then used model outputs to compute the magnitude of decadal trends in seasonal and annual Tw
75 and Q. To understand the relative influences of Q and Ta on Tw, we compared their trends, anomaly behaviors, and temporal patterns. Finally, we sought to understand variation in Tw trends as a function of stream size, landscape attributes, and riparian shading.

2 Study area

The Loire River basin is one of the largest in Europe (10^5 km^2) encompassing an area with starkly contrasting HydroEco
80 Regions ("HER"), land use/land cover, and climatic conditions (Moatar and Dupont, 2016), providing an ideal case study to disentangle the drivers of the spatial heterogeneity of trends in Tw. Mean annual precipitation (549–2130 mm), mean annual Ta (6.0–12.5 °C), and altitude (10–1850 m) provide spatially variable controls on stream thermal regimes. There are three main HER in this basin (Fig. 1, middle), which were categorized based on climate, lithology, and relief (Wasson et al., 2002). Granite and basalt dominate the southern headwaters of the basin (mostly in the Massif Central, HER A), whereas sedimentary
85 rocks occupy the middle reaches with a potential for groundwater input (HER B), followed by granite and schist in the lower reaches (HER C) (see Fig. 1, top).

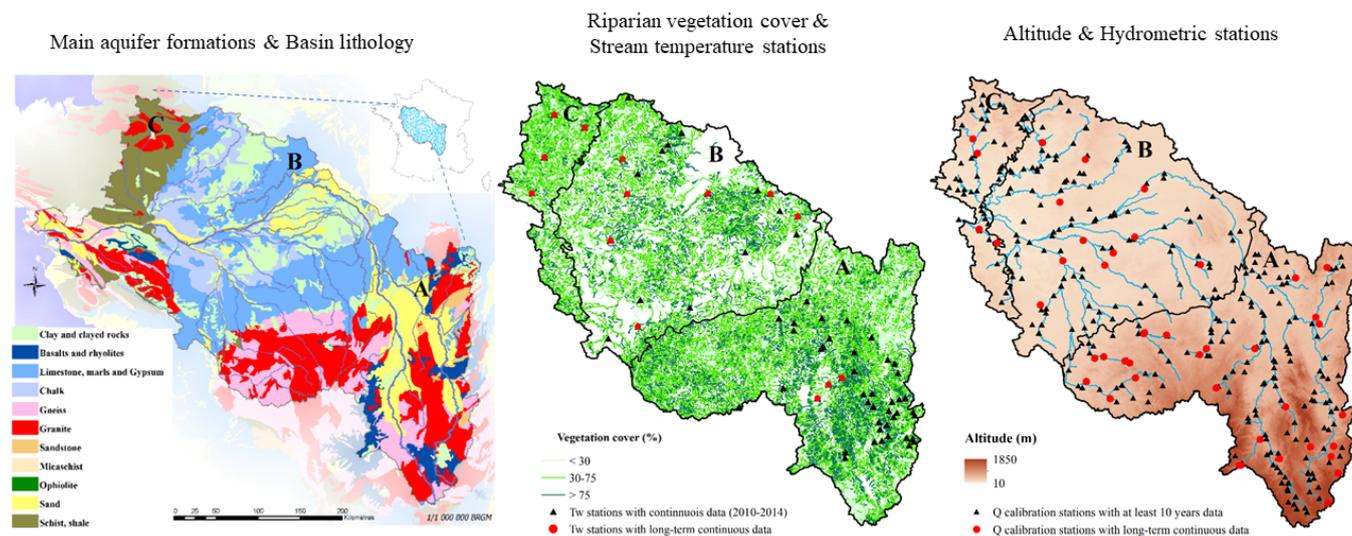


Figure 1. Maps of the Loire basin. (top) Main aquifer formations and lithology, (middle) riparian vegetation cover (Valette et al., 2012) and Tw stations, and (bottom) altitude (IGN, 2011) and hydrometric stations. The lithology map was adapted from Moatar and Gailhard (2006), based on original data from BRGM (French Geological Survey). All Tw stations were used to assess the performance of the T-NET thermal model, but only the ones with long-term data (in red) were used to assess the model accuracy for long-term trends. Complete information on Tw stations with long-term continuous data are provided in Table 1. All hydrometric stations were used for calibrating the EROS hydrological model, but only stations with long-term data (in red) were used to assess the model performance on long-term trends.

3 Method and data

We assessed how Tw responded to climate change over the past 57 years in the Loire River basin in four steps. First, we applied physically based Q and Tw models for the period 1963–2019. Second, we assessed model performance by comparing simulated
90 daily Q and Tw to data from observation stations. Third, we assessed Q and Tw long-term trends. Fourth, we analyzed how hydro-climatic changes and landscape features could explain reconstructed trends in Tw. We performed all analyses on both seasonal and annual basis, where winter is December–February (DJF), spring is March–May (MAM), summer is June–August (JJA), and fall is September–November (SON).

3.1 Modeling daily Q and Tw

95 3.1.1 EROS hydrological model

The EROS hydrological model uses daily T_a ($^{\circ}\text{C}$), solid and liquid precipitation (mm), and reference evapotranspiration (ET_0 , mm) to produce mean daily Q and groundwater flows (Thiéry, 1988; Thiéry and Moutzopoulos, 1995; Thiéry, 2018). Meteorological inputs were provided by the 8 km gridded Safran atmospheric reanalysis data released by Météo-France over



the 1958–2019 period (Quintana-Segui et al., 2008; Vidal et al., 2010). ET_0 was computed from Safran variables with the
100 Penman-Monteith equation (Allen et al., 1998). Observed Q data were extracted from the French national Banque Hydro
database (<http://www.hydro.eaufrance.fr/>) for all available stations across the Loire basin (Fig. 1, bottom). Stations along the
main Loire and Allier rivers were highly influenced by the management of large dams, notably through summer releases to
sustain low-flows. Time series at these stations have been first naturalized by EDF (French Electricity) by taking into account
recorded dam storages and releases. EROS was calibrated over the 1971–2018 period against daily Q at 352 sub-catchments
105 (range=40–1600 km², mean=300 km²) with at least 10 years of daily observations (Fig. 1). The calibration aimed at maximiz-
ing the Nash-Sutcliffe efficiency criteria (Nash and Sutcliffe, 1970) on the square root of streamflow and minimizing the overall
bias, in order to simulate correctly the whole range of Q values (Thiéry, 1988; Thiéry and Moutzopoulos, 1995; Thiéry, 2018).
A 3-year warm-up period (1971–1974) was discarded from the calibration period (1971–2018, which maximizes the amount
of streamflow observations). The calibrated model was then used to simulate streamflow over 368 sub-catchments in the Loire
110 basin over the whole 1963–2019 period. Streamflow was then distributed along the river network according to the drainage area
for informing the T-NET model at the reach scale. Although meteorological variables were available from 1958, the first three
years (1958–1962) was discarded for the sake of model convergence.

3.1.2 T-NET thermal model

The T-NET (Temperature-NETwork) thermal model computes T_w along the longitudinal dimension of the hydrographic net-
115 work (a GIS polyline) of the Loire River basin. To simulate T_w , the equilibrium temperature (T_e) is first computed, the temper-
ature at which the net heat flux across the surfaces of the stream is null (Bustillo et al., 2014). The heat budget of each reach
includes six fluxes (Wm^{-2}): net solar radiation, atmospheric longwave radiation, longwave radiation emitted from the water
surface, evaporative heat flux, convective heat flux, and groundwater heat inflow. The hydrographic network of the model over
the Loire basin consists of 52 278 reaches delimited either by confluences of two streams or a headwater source (i.e., first order
120 reaches) (Beaufort et al., 2016; Loicq et al., 2018). The mean reach length is 1.7 km and 74 % of the reaches have a Strahler
order lower than 3. To compute the six heat fluxes and the water travel time for each reach, the following input data were used:

- Meteorological variables: hourly T_a (°C), specific humidity (gkg^{-1}), wind velocity (ms^{-1}), shortwave radiation (Wm^{-2})
and longwave radiation (Wm^{-2}) were provided by the 8 km gridded Safran atmospheric reanalysis (Vidal et al., 2010).
All reaches within a grid cell were assigned the values of the meteorological variables in that grid cell. For reaches flow-
125 ing through more than one grid cell, meteorological variables were weighted by the relative length of the reach within
each grid cell.
- Riparian vegetation shading: riparian vegetation is one of the major regulators of shortwave radiation. In the current
study, patches of wooded area provided by the BD TOPO® (IGN, 2008) database were used as a proxy of vegetation.
The vegetation species and length of each wooded patch in a buffer of 10 m were extracted for both right and left river
130 banks (van Looy and Tormos, 2013). The vegetation density (vc) was then calculated as the ratio of patch length to
reach length for both right and left river banks. In case of multiple wooded patches in any side of a river bank, the



average vegetation density of the patches was considered. Then, the model proposed by Li et al. (2012) was used for the calculation of the dynamic shading factor (SF). The required average tree height for both right and left river banks was estimated based on vegetation species (see Table S1).

135 In the presence of different vegetation species, the average tree height (m) for each side of a river bank was calculated as follows:

$$H = \frac{1}{n} \sum_{i=1}^n H_i \frac{L_i}{L} \quad (1)$$

with H_i and L_i the height and length of the tree patch i , respectively, and L the reach length. Next we calculated the proportion of the river width that was shaded (W_{shaded}) and the dynamic shading factor (SF) as follows:

140
$$W_{\text{shaded}} = \frac{H_{\text{left/right}} \times \cot \Psi \times \sin \delta}{W} \quad (2)$$

$$SF_{\text{right}} = (W_{\text{shaded}})_{\text{right}} \times (vc)_{\text{right}} \quad (3)$$

$$SF_{\text{left}} = (W_{\text{shaded}})_{\text{left}} \times (vc)_{\text{left}} \quad (4)$$

$$SF = \begin{cases} SF_{\text{left}} & \text{if } SF_{\text{left}} > SF_{\text{right}} \\ SF_{\text{right}} & \text{otherwise} \end{cases} \quad (5)$$

145 where H is the average tree height (see Eq. 1), W the river width (see Eq. 7), Ψ the solar altitude angle, δ the angle between solar azimuth and the mean azimuth of T-NET reach, and vc the vegetation density. To take into account the phenology and stages of leaf growth, a coefficient corresponding to each season and transmissivity was applied to SF to calculate the final shading factor: $SF_{\text{final}} = SF \times (1 - \text{transmissivity})$. The transmissivity in leafless months (Jan, Feb, Nov and Dec), months of leaf growth (Mar and Apr), and full-leaf months (May-Sep) was fixed to 0.3, 0.2 and 0, respectively, following Hutchison and Matt (1977). The shortwave radiation was lastly regulated by a factor of

150 $1 - SF_{\text{final}}$.

– River hydraulic geometry: stream width and depth were calculated using a hydraulic model assuming a rectangular river section being constant over 24 hours (Morel et al., 2020):

$$D(t) = D50 \times \left[\frac{Q(t)}{Q50} \right]^f \quad (6)$$

$$W(t) = W50 \times \left[\frac{Q(t)}{Q50} \right]^b \quad (7)$$

155 with f and b being at-a-reach exponents previously predicted by climate, hydrological, topographic and land use descriptors (see Morel et al., 2020, for more details). $Q(t)$ is the daily mean streamflow provided by the EROS hydrological model. The $Q50$, $W50$, $D50$ (the median of Q , width and height, respectively) and the exponents were available on the Theoretical Hydrographic Network for France (RHT, Pella et al., 2012). There was about 50 % correspondence between the reaches of the T-NET and RHT networks. For the rest of them, required hydraulic geometry variables for the T-NET



160 reaches were extrapolated from the nearest RHT reach. These river hydraulic geometries allowed us to calculate the water velocity by the ratio of $Q(t)$ to rectangular wetted cross-section. The travel time was also defined by the ratio of water velocity to reach length.

3.2 Model assessment and validation

3.2.1 EROS hydrological model

165 Of the 352 calibration stations considered by EROS, 44 are part of the French Reference Hydrometric Network (RHN) described by Giuntoli et al. (2013) with long-term continuous high-quality data over the 1968–2019 period, especially for low-flows. These stations are shown with red points in Fig. 1. Seasonal and annual relative biases, together with Nash-Sutcliffe efficiency on Q , $\ln(Q)$, and \sqrt{Q} were computed over the 1968–2019 period on these RHN stations to provide an overview of the performance of the EROS model. Moreover, decadal trends (in % per decade) on seasonal and annual averages from the
170 EROS simulation were compared to corresponding observed trends at each of the 44 reference stations.

3.2.2 T-NET thermal model

The T-NET model does not consider the influence of impoundments on thermal energy balance, and thus produces "natural" thermal regimes. Therefore, model performance was assessed on natural T_w stations, which are weakly influenced by impoundments. 72 near-natural stations with continuous daily data over the 2010–2014 period (see Fig. 1) were identified using
175 the thermal signatures approach that allows distinguishing between natural and altered thermal regimes (see Seyedhashemi et al., 2020, for more details). Of these identified natural reaches, 58 were located on small/medium streams (with distance from the source <100 km), while the remaining are located on large rivers. The mean catchment area of natural stations was $153 \text{ km}^2 (\pm 225 \text{ km}^2)$ for small/medium streams, and $16,804 \text{ km}^2 (\pm 18,833 \text{ km}^2)$ for large rivers. Seasonal and annual absolute biases were assessed at these 72 stations.

180 Long-term continuous data was available at 14 of the 72 near-natural stations, including 9 stations with 8–13 years data and 5 stations with 20–40 years data. These 14 stations are represented as red points in Fig. 1, middle), and listed in Table 1. The long-term evolution of annual mean T_w at these stations is shown in Fig. S1. These 14 near-natural stations with long-term continuous data comprise the validation dataset for the seasonal and annual trend assessment (see Table 1).

3.3 Time series reconstruction and assessment of long-term trends

185 Daily Q and T_w were reconstructed over the 57-yr period 1963–2019 using the EROS hydrological model and the T-NET thermal model. For each of the 52 278 river reaches, daily time series of T_a (from the Safran reanalysis), Q (from EROS), and T_w (from T-NET) were reconstructed. Seasonal and annual averages of these 3 variables were considered in the trend assessment.

We estimated the magnitude of trends in these time series with the non-parametric Theil–Sen estimator (Sen, 1968), and
190 evaluated their significance with the Mann-Kendall test (Mann, 1945), commonly used in hydrological analyses (see e.g.



Table 1. Characteristics of the 14 long-term Tw stations. See Fig. S1 for the evolution of observed annual Tw at these stations.

River (Location)	Catchment area (km ²)	Record period	Total years
Loire (Chinon)	57043	1977–2019	43
Loire (St-Laurent)	38088	1977–2019	43
Loire (Dampierre)	36212	1977–2019	43
Loire (Belleville)	35172	1979–2019	41
Vienne (Civaux)	5795	1997–2017	21
Artière (Clermont-Ferrand)	48	2005–2017	13
Oudon (Segré)	1342	2004–2014	11
Mayenne (Ambrières-les-Vallées)	825	2004–2014	11
Bedat (Saint-Laure)	419	2008–2017	10
Credogne (Puy-Guillaume)	84	2008–2017	10
Loir (Flée)	6215	2010–2017	8
Huisne (Montfort-le-Gesnois)	1931	2010–2017	8
Jouanne (Forcé)	413	2010–2017	8
Merdereau (Saint-Paul-le-Gaultier)	123	2010–2017	8

Giuntoli et al., 2013) but also thermal analyses (e.g. Kaushal et al., 2010; Arismendi et al., 2013a; Arevalo et al., 2020). This test is robust to non-normal data, non-linear trends, and series with outliers and missing values. Trend magnitudes are reported in °C/decade for Ta and Tw, and in %/decade for Q (percentage of changes over whole period), to help for comparisons across the basin.

195 3.4 Hydroclimatic drivers of Tw trends

Distributions of trends in Tw and Ta were first compared for the whole basin at the seasonal and annual scales using the non-parametric Wilcoxon signed rank test (Bauer, 1972) to determine whether Tw trends were greater than Ta trends. To assess how Ta and Q influenced Tw, we first identified which reaches exhibited 1) jointly increasing trends in Tw and Ta, and 2) jointly increasing trends in Tw and Ta and decreasing trends in Q. Then, for each identified reach, we evaluated the strength and direction of these joint trends using Pearson correlation between 1) Tw and Ta, and 2) Tw and log(Q).

Ta, Tw, and Q seasonal and annual anomalies – with respect to the 1963–2019 interannual mean – were then used to synchronicity of extreme years. Change-points in time series of anomalies at each reach were computed with the non-parametric Pettitt test that considers no change in the central tendency as a null hypothesis (Pettitt, 1979). Change points were reported at the 95 % confidence level.



205 3.5 Landscape drivers of Tw trends

Stream size and HER (see Fig. 1) were selected as the major potential landscape drivers. The Strahler order of each reach was used as a proxy for stream size. Reaches with Strahler order 5–8 were combined into a single group termed "large rivers". The Spearman correlation was computed between median decadal trends in Tw (i.e., median across all reaches) and Strahler order. Such correlations were computed across HERs and at seasonal and annual scales to evaluate the spatial heterogeneity and seasonality.

Lastly, the influence of riparian vegetation shading on trends in Tw was assessed using the daily average of the riparian vegetation shading (SF) simulated by T-NET. Seasonal shading was computed as the average of the daily SF over each season. For this analysis, only low-order reaches – distance from the source < 30 km – were considered, based on previous observations that riparian shading primarily influences Tw at this scale (Dan Moore et al., 2005; Loicq et al., 2018). Then, as for the previous analysis for the influence of stream size, the correlation between median decadal Tw trends and five levels of riparian shading (<15 %; 15-25 %; 25-40 %; 40-60 %; >60 %) was computed across HERs and seasons.

4 Results

4.1 Performance of models against observations

The EROS model performed well at the annual scale with a median relative bias of 0.37% (see Fig. S2). It slightly underestimated winter Q (median bias=-7.26%) and spring Q (-6.79%), and overestimated summer Q (+37.7%) and fall Q (+24.7%). The mean NSE criteria for low, mean and high flows were 0.82, 0.85 and 0.79, respectively. No systematic bias was observed for modeled Tw at the stations located on small and medium rivers (see Fig. S2). Median Tw bias ranged from -0.26 °C (in fall) to 0.8 °C (in winter). Large rivers exhibited a small Tw underestimation, with a median bias ranging from -0.29 °C (in fall) to +0.15 °C (in winter), and the overall biases were still quite small across seasons (IQR=0.4–0.7 °C).

Trends in observed and modeled Q were well correlated for all seasons (Fig. S3), with the highest correlation across stations found in spring ($r = 0.69$, $p < 0.05$) and the lowest correlation found in summer ($r = 0.17$, $p = 0.26$). Both modeled and observed Q were slightly decreasing (up to -11 %/decade) for the majority of stations across all seasons, but the trend was significant for a very few of them (and mostly at the annual scale), all located in the southern headwaters in HER A (red points of Fig. S3). Moreover, there were only a few discrepancies between estimates of trend significance in modeled and observed Q across seasons (11-18 % of stations).

Modeled and observed Tw trends correlated well (see Fig. S4) across seasons, with the highest correlation in summer ($r = 0.94$, $p < 0.05$) and the lowest correlation in fall ($r = 0.29$, $p = 0.32$). Contrasting with trends in Q, trends for Tw increased for most stations across seasons, but the short period of record led to mostly non-significant ($p=0.05$) trends. However, stations with long-term data showed significant increasing trends for all seasons, with the exception of winter (Fig. S4). A visual comparison of observed and modeled Tw time series at stations with long-term data indeed suggested a strong coherence and agreement between observations and simulations for all seasons (Fig. 2). For the four stations along the main stem of the Loire

river (Fig 2), the greatest increase occurred in spring – +0.61 (resp. +0.71) °C/decade in observations (resp. simulations) – and summer – +0.62 (resp. +0.58) °C/decade in observations (resp. simulations).

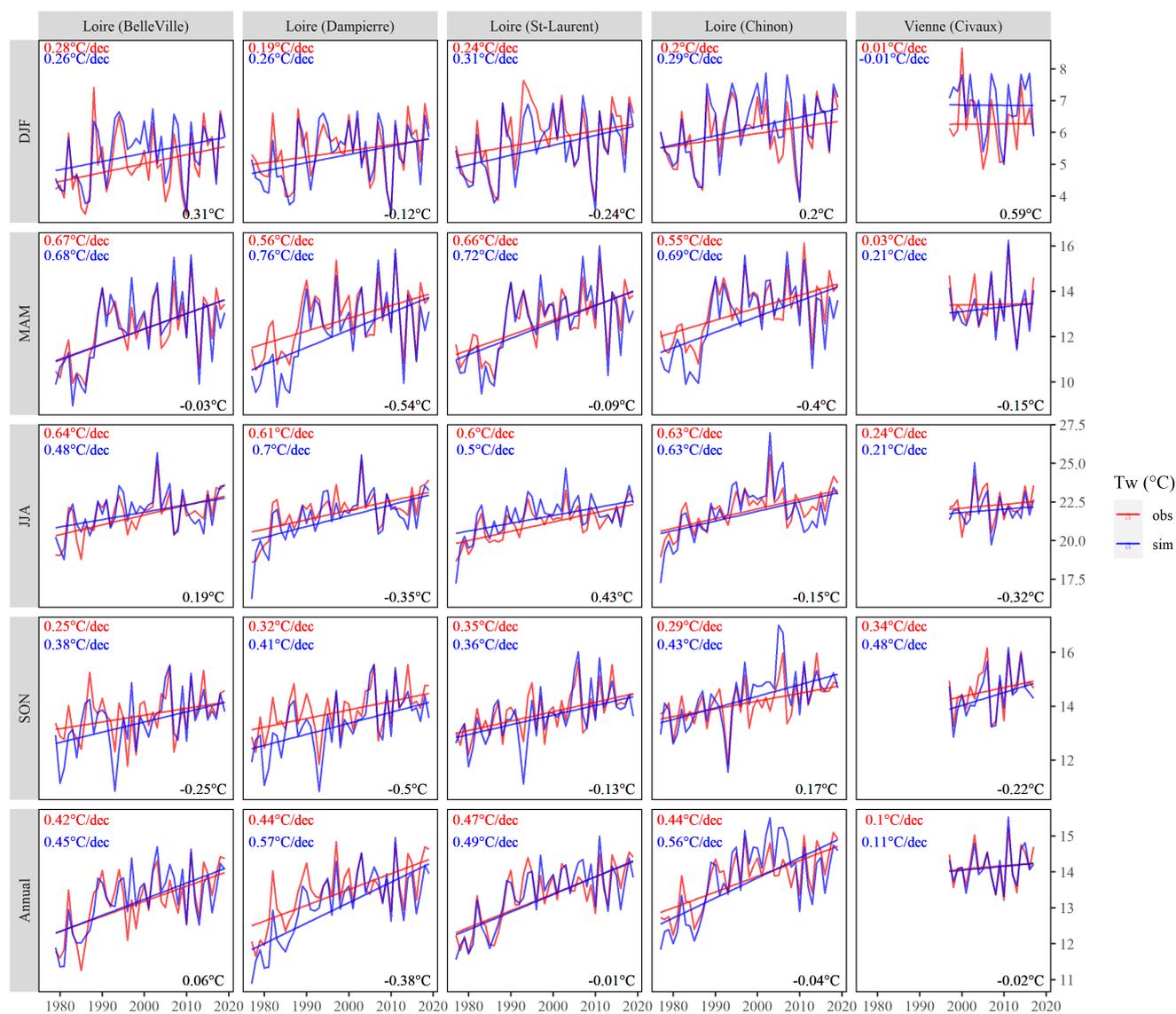


Figure 2. Seasonal and annual time series of observed and simulated Tw at stations with long-term continuous data (see Table 1 for more information) between 1977 and 2019. Numbers in red and blue in the top left corner of each graph show trend values (Sen’s slope) in observed and simulated Tw. Numbers in black in the bottom right corner of each graph show the mean bias of the reconstruction.



4.2 Spatial reconstruction of long-term trends

240 Tw increased in almost all modeled reaches for all seasons (Fig. 3, left; Fig. S5). Depending on the season considered, 62 % to 80 % of reaches showed trends in the range of +0.2- +0.4 °C/decade (i.e 1.14-2.28 °C over the whole 1963-2019 period). Summer Tw trends were more spatially variable than in other seasons, with more than 50 % of reaches showing values higher than +0.4 °C/decade (see Fig. S6). Such reaches were mainly located in the southern part of the basin, in HER A (see Fig. 3, left). Spring Tw trends showed a similar spatial pattern, but with lower trend values.

245 Likewise, Ta exhibited increasing trends for 99 % of all reaches across spring, summer, and the whole year (Fig. 3, middle). Values were mainly in the range of +0.2- +0.4 °C/decade (see Fig. S6). The highest Ta trend values were found in summer (resp. spring), when 67 % (resp. 22 %) of reaches showed values higher than +0.4 °C/decade. Such reaches were mainly located in HER A, especially in summer. Non-significant trends were found over the whole basin in winter, and in the southern part of the basin in fall.

250 In contrast to Ta and Tw, trends in Q were highly variable in magnitude and direction across the basin and across seasons (Fig. 3, right), and most were not significant at $p=0.05$ (Fig. S5). However, significant decreasing trends were found in the southern headwaters (HER A) in spring, summer, fall, and annual scale (Fig. S5). Decreasing trends were observed for the majority of reaches across seasons (66-83% of reaches), with the exception of winter (37%). Decreasing trends could have magnitudes greater than -5 % per decade, implying a -28 % loss in Q over the whole 1963-2019 period.

255 4.3 Hydroclimatic drivers of Tw trends

Relationships between trend estimates

The median of Tw trends were higher than that of Ta trends for every season ($p<0.001$ according to the Wilcoxon signed rank test), except for summer when the median trend values for Tw and Ta were very similar, but more variable for Tw (+0.08- +1.02 °C/decade) (Fig. 4). The greatest increase in Tw was found in summer (+0.44 °C/decade). Overall, Tw trends were
260 more spatially variable than Ta trends, suggesting the conditional influence of Q trends (Fig. 4). Indeed, where Tw trends exceeded Ta trends, decreasing Q trends occurred coincidentally at the majority of reaches for all seasons – with the exception of winter – (43-72 %, depending on season; Fig. 5). Of these specific reaches where all factors converged (trend in Tw higher than trend in Ta, and decreasing trend in Q), most were located in HER A, especially in spring (52 % of such reaches) and summer (79 % of such reaches).

265 Synchrony of annual anomalies

We observed strong positive correlations between seasonal and annual averages of Tw and Ta across seasons (see Table 2). We further observed strong negative correlation between summer Tw and Q time series. The strong positive correlation observed between winter Ta and Q results from the particular hydroclimate of winters in the Loire basin, where they are either either warm and wet or cold and dry.

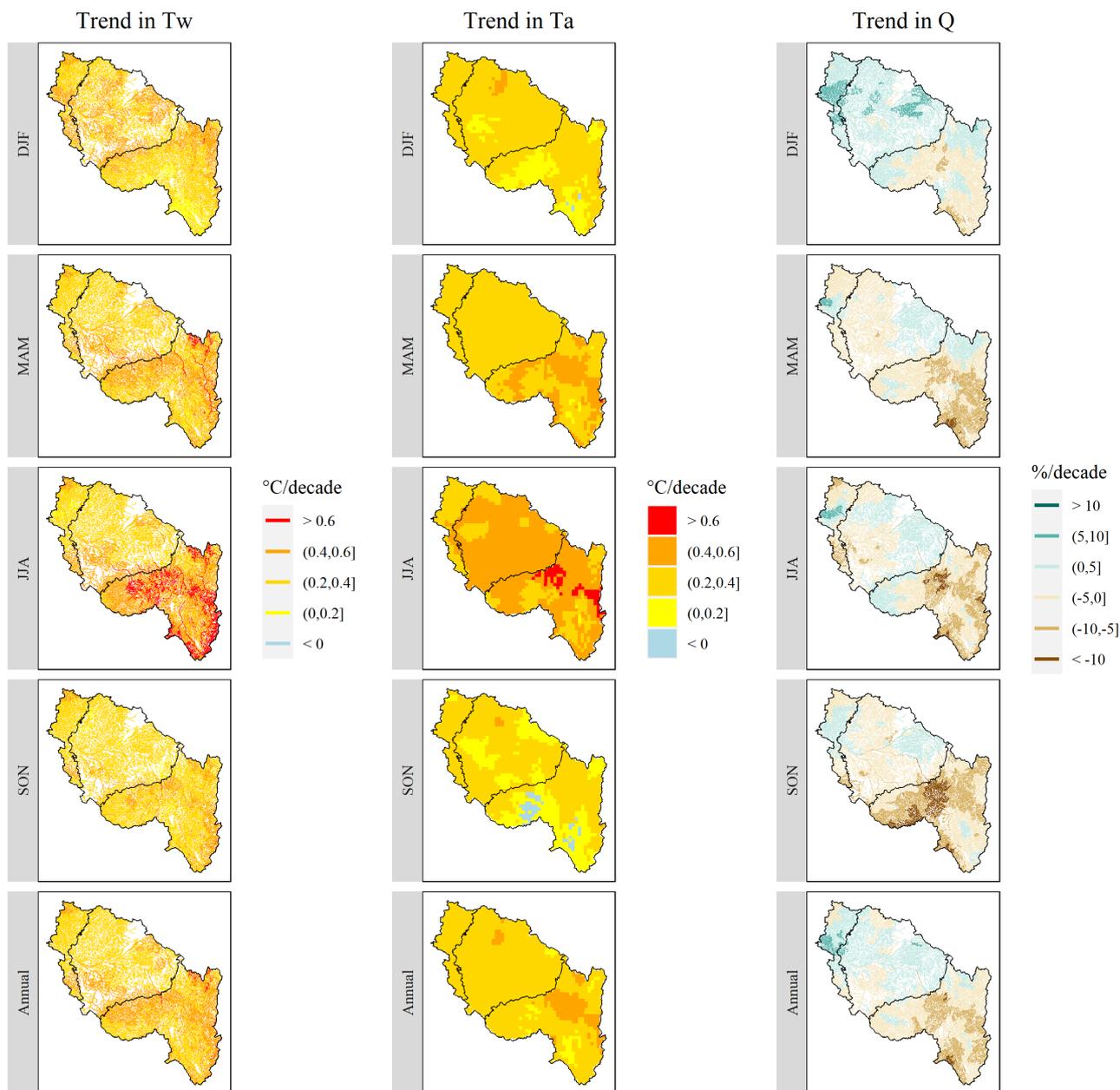


Figure 3. Spatial variability of trends in seasonal and annual Tw, Ta and Q over the 1963-2019 period, based on the Sen's Slope estimator. Solid black lines show the Hydro-Ecoregion (HER) delineation (see Fig. 1). The statistical significance of these trends is given in Fig. S5.

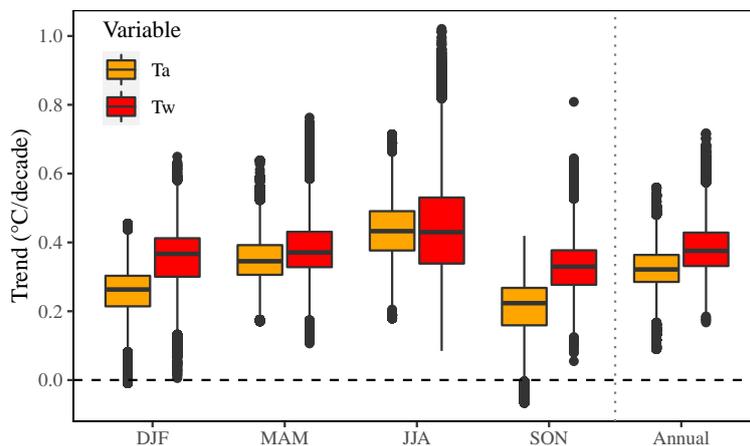


Figure 4. Distributions of seasonal and annual trends in Tw and Ta for all 52 278 reaches over the 1963-2019 period. Sen’s slope is used as trend value estimate (see text).

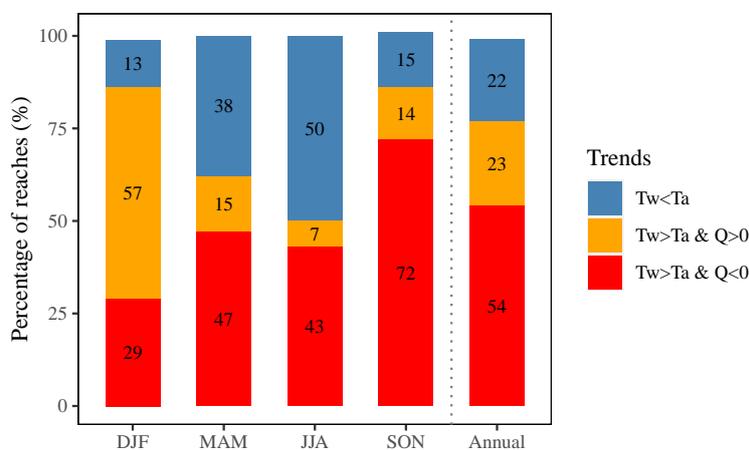


Figure 5. Percentage of reaches with consistent 1963-2019 trends in Tw, Ta, and Q, categorised with respect to two criteria: (1) Tw trend > Ta trend, and (2) sign of Q trend. Sen’s slope is used as trend value estimate.

270 Annual anomalies of Tw, Ta, and Q exhibited variable patterns, with Tw and Ta generally increasing and Q remaining relatively stationary (Fig. 6). Tw anomalies were generally more variable than Ta, especially in summer, but both time series appeared to exhibit synchronous behavior. Change-point analysis supported this visual observation, where change-points in seasonal and annual averages were largely coincident across these time series (Fig. 7). Tw and Ta anomalies exhibited clear negative-to-positive change-points in the late 1980s at nearly all reaches, with median values shifting by approximately +2 °C.

275 These change points were observed in all seasons, but were most pronounced and synchronous around 1988 in spring and summer. The change-points detected in winter Tw and Ta time series were less concomitant, occurring mostly in the early

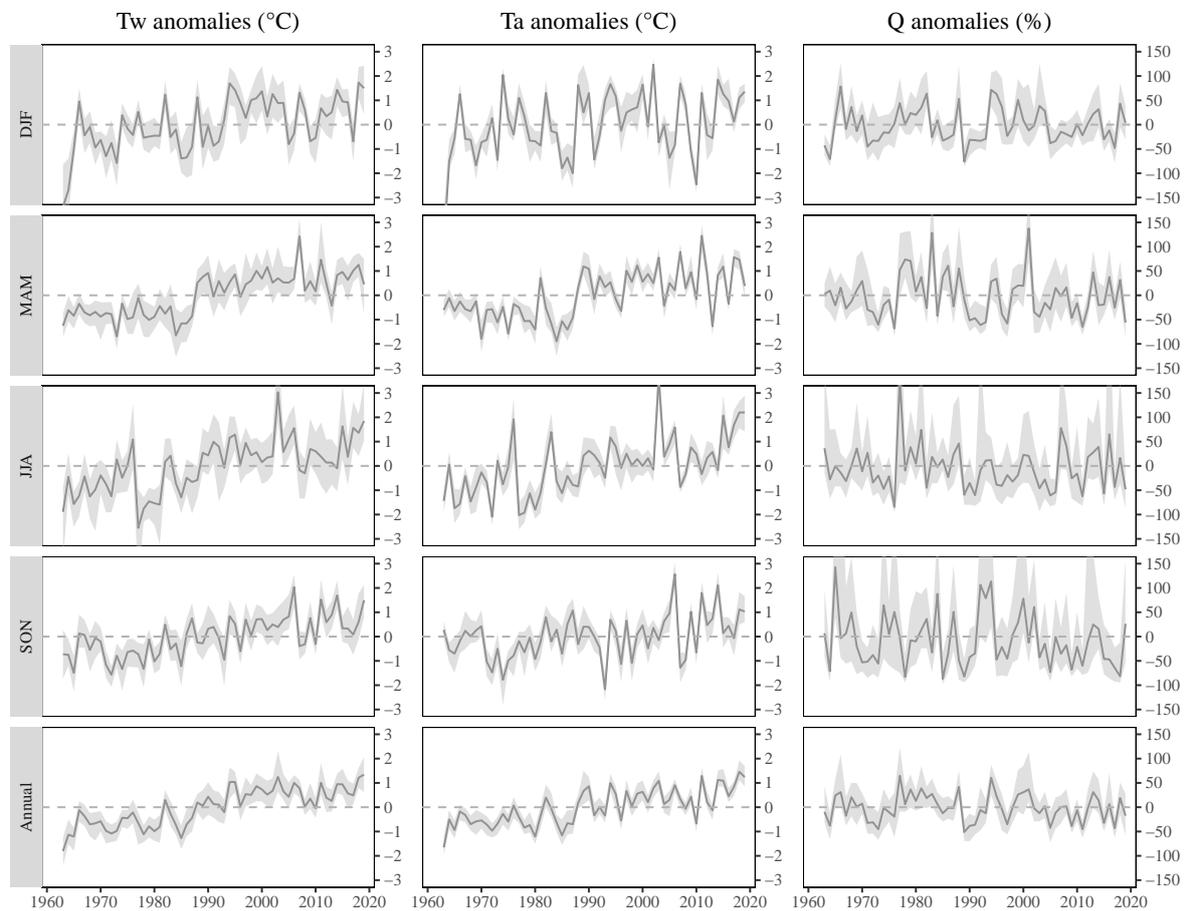


Figure 6. Seasonal and annual times series of anomalies in Tw ($^{\circ}\text{C}$), Ta ($^{\circ}\text{C}$) and relative Q (%) with respect to 1963–2019 averages. Grey intervals show the 5th and 95th percentiles across reaches, and the solid grey line depicts the median value. Note that Ta and Tw have the same scale.



Table 2. Pearson correlation over the 1963–2019 period between seasonal and annual Tw and Ta and/or log-transformed Q time series, averaged over all reaches. Percentages in brackets show the proportion of reaches with a significant correlation at the 95 % confidence level.

Season	Tw and Ta	Tw and log(Q)
DJF	+0.73 (100%)	+0.52 (94%)
MAM	+0.78 (100%)	-0.02 (25%)
JJA	+0.82 (100%)	-0.40 (79%)
SON	+0.72 (99,6%)	-0.01 (19%)
Annual	+0.83 (100%)	-0.01 (22%)

1990s (1992 and 1993) for Tw and in the late 1980s (1986–1989) for Ta. The fall change-points were distributed between 1980 and 1994 for both Tw and Ta. The significant change-points in seasonal Q time series were detected for a substantially smaller proportion of reaches, e.g. less than 40 % of reaches for spring and summer. The majority of these reaches were located in
280 HER A across seasons (66–86 % of such reaches), with the exception of winter (49 %) (see Fig. S8). In spring and summer, they occurred in the late 1980s, similarly to Tw and Ta. Conversely, the significant change-points detected in other seasons were much more scattered in time, probably due to the high interannual variability of Q.

Critically, the largest summer Tw and Ta positive anomalies over the study period were observed in 1976, 2003, 2006, 2015, 2017, and 2019, which corresponded to years with the largest negative anomalies in summer Q (Fig. 8). Note that this signal
285 was much less clear for the other seasons (see Fig. S9).

4.4 Landscape drivers of Tw trends

4.4.1 Stream size and HER

Strahler order was strongly and positively correlated with Tw trends in spring and summer, but this effect was modulated by HER, with HER A exhibiting the strongest correlations (Fig. 9). In other words, larger rivers tended to exhibit the largest
290 increases in spring and summer Tw, especially for reaches located in the HER A. There, median trends in spring (resp. summer) ranged from +0.37 (resp. +0.49) °C/decade for small streams (Strahler order 1) to +0.55 (resp. +0.64) °C/decade for large streams (Strahler order ≥ 5).

4.4.2 Riparian shading

For small streams, i.e. reaches located closer than 30 km from the source, the shading factor SF and median trends in Tw
295 were significantly and negatively correlated for all three HERs in spring, as well as for HER A in summer and at annual scale (Fig. 10). The highest correlation was found in summer in HER A. Unsurprisingly, the influence of riparian vegetation shading on trends in Tw was more important in spring and summer. The mitigating effect of shading on trends in Tw for small streams was observed for all HERs in spring, and only for HER A in summer and, to a lesser extent, in fall. The median spring Tw trend

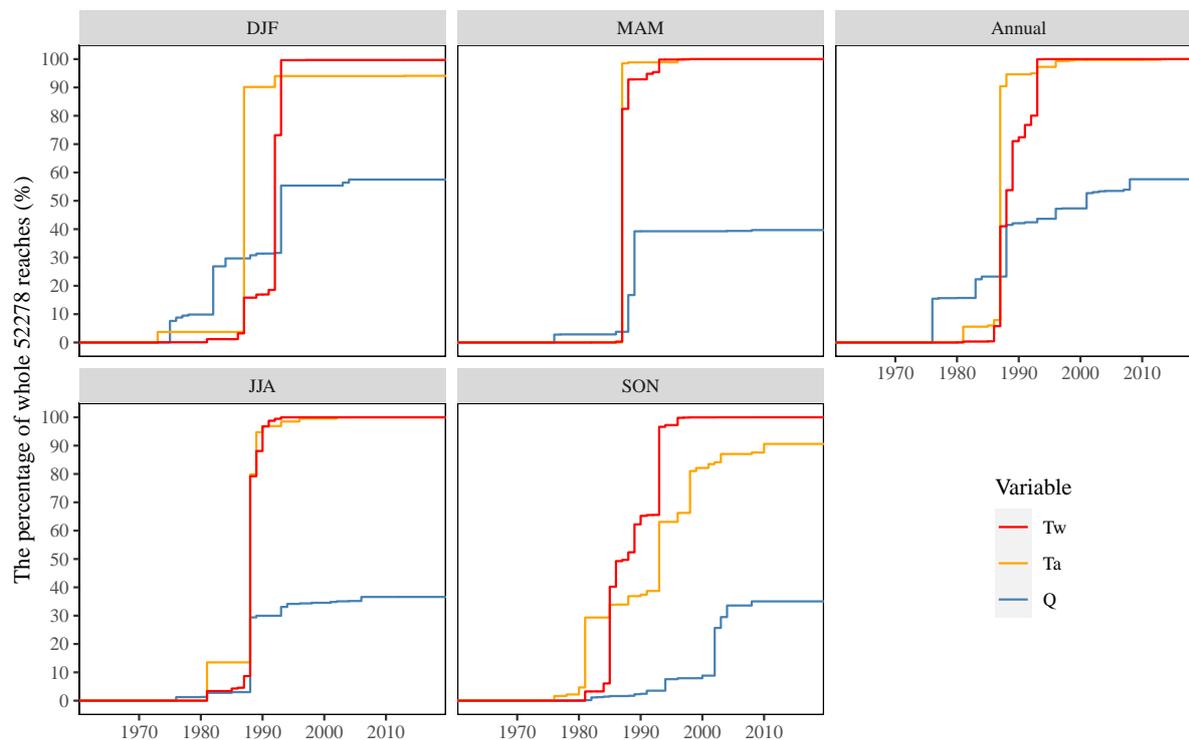


Figure 7. Change-point in Tw, Ta, and Q time series at the seasonal and annual scales, plotted as a proportion of reaches experiencing a shift in a given year. Only the first change-point detected at the 95% confidence level is considered, and non-significant change-points were removed, leading to curves not reaching 100 %.

in the HER A, B and C decreased by 12 %, 5 % and 4 %, respectively, from sparsely shaded reaches ($SF < 15\%$) to highly shaded reaches ($SF > 40\%$). For summer Tw in HER A, the median trends were 16 % lower between the lowest and highest shaded reaches.

5 Discussion

5.1 Quality and suitability of simulated Tw and Q

Although some biases were observed for both Q and Tw (Fig. S2), we found high correlations between modeled and observed trends in seasonal and annual Q, with the exception of summer (Fig. S3), and Tw, with the exception of fall (Fig. S4), demonstrating the adequacy of the modelling approach for temporal trend analyses. For Q, although largely non-significant (Fig. S5), decreasing trends were observed for the majority of the reaches across seasons (66-83% of reaches, with the exception of winter, Fig. S7) strongly suggested an effect on Tw. Moreover, the spatial pattern in simulated Q trends, with significant decreases



Table 3. Recent studies on Tw trends in Europe. A comprehensive review of the relevant literature published prior to 2016 can be found in Arora et al. (2016). Magnitudes with unspecified season are related to annual scale. Notice that except present study, the others used observed Tw.

Country	Sites	Period	Rate of change (°C/decade)	Reference
France	52278 reaches in the Loire basin	1963–2019	+0.17– +0.72 (Mean=+0.38) +0.01– +0.65 (+0.35) in winter +0.11– +0.76 (+0.38) in spring +0.08– +1.02 (+0.44) in summer +0.05– +0.81 (+0.33) in fall	Present study
Austria	18 rivers	2010-2017	+1.9– +3.2 in summer	Niedrist and Füreder (2021)
England	6148 sites	2000-2018	-0.4	Wilby and Johnson (2020)
Switzerland	31 rivers	1979-2018	+0.33 (±0.03) +0.6– +1.1 in summer	Michel et al. (2020)
Poland	5 Carpathian rivers	1984–2018	+0.33– +0.92 +0.82– +0.95 in spring +0.75– +1.17 in summer +0.51– +1.08 in fall +0.25– +0.29 in winter	Kędra (2020)
France	11 stations on Loire, Vienne, Rhône, Seine, Meuse	1980-2015	+0.79 in spring	Maire et al. (2019)
Poland	6 stations on Warta River	1960-2009	+0.096– +0.28	Ptak et al. (2019a)
Croatia	6 stations on Kupa River	1990-2017	+0.23– +0.796	Zhu et al. (2019)
Switzerland	Rhine, Rhône, Aar, and Thur rivers	1983-2013	+0.27 (± 0.03)	Zobrist et al. (2018)
Northern Germany	132 sites	1985-2010 1985-1995	+0.3 (±0.03) +0.69 (±0.10) in spring +0.78 (±0.06) in summer +0.75 (±0.09) in fall +0.39 (±0.23) in winter +0.81 (±0.2)	Arora et al. (2016)
England and Wales	475 sites 2773 sites	2000-2010 1990–2006	+0.9 (±0.07) +0.3 (±0.02)	Orr et al. (2015)
Poland	Coastal rivers (Rega, Parsęta, Słupia, Łupawa, Łeba)	1971-2015	+0.26– +0.31 +0.46 in April (The month with the highest trend)	Ptak et al. (2016)
France	4 stations on Loire River	1976–2003	+0.61– +0.71 18 +0.86– +1.07 in spring and summer	Moatar and Gailhard (2006)

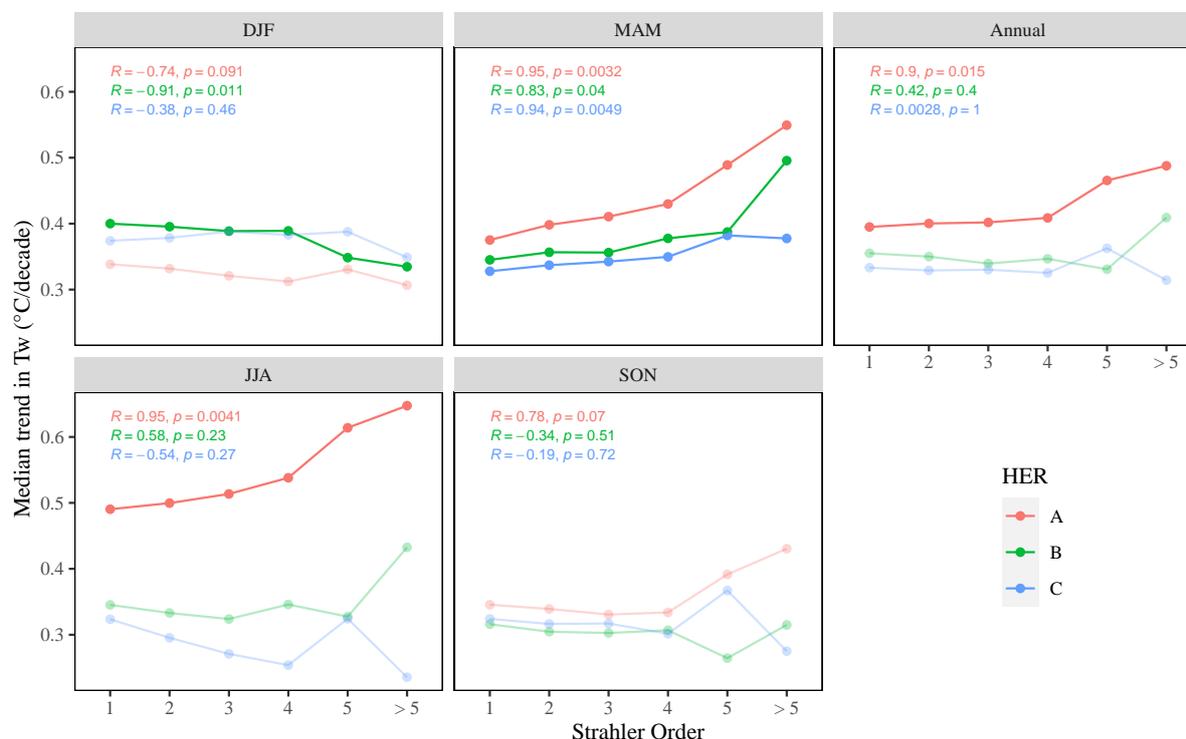


Figure 9. Relationships between reach size and median trends in Tw across reaches over 1963-2019, by HER and by season. Correlations and associated p-values are shown in the top-left corner of each graph, and significant relationships at the 95 % confidence level are identified by full solid lines.

Global-scale stream temperature modelling suggests trends in annual averages ranging from +0.2 to +0.5°C/decade over France (Wanders et al., 2019), which is consistent with our findings (mostly in the range of +0.2- +0.4°C/decade, Fig. S6). We found more pronounced trends in spring and summer, which was also found in other parts of Europe (e.g Kędra, 2020; Arora et al., 2016; Michel et al., 2020). Considerable discrepancies were also found between Tw and Ta trends across seasons for the majority of the reaches (see Fig. 3, and 5), which is a common finding for other sites around the world (Arora et al., 2016; Wanders et al., 2019). This highlights that changes in Ta may not be the only driver of changes in natural Tw.

5.3 Drivers and spatial patterns of trends in Tw

The greatest increases in Tw (up to +1 °C/decade) were predominately located in the southern headwaters of the basin, in HER A (Massif Central) where a greater increase in Ta (up to +0.71 °C/decade) and a greater decrease in Q (up to -16 %/decade) occurred jointly. The decrease in Q could be due to a significant increase in potential evapotranspiration (PET) (up to +10 %) over the whole of basin and a decrease in total precipitation (P) (up to -5 %/decade) (Figs. S10 and S11). Such trends, computed here based on variables from the Safran surface meteorological reanalysis (Vidal et al., 2010), are consistent with larger-scale

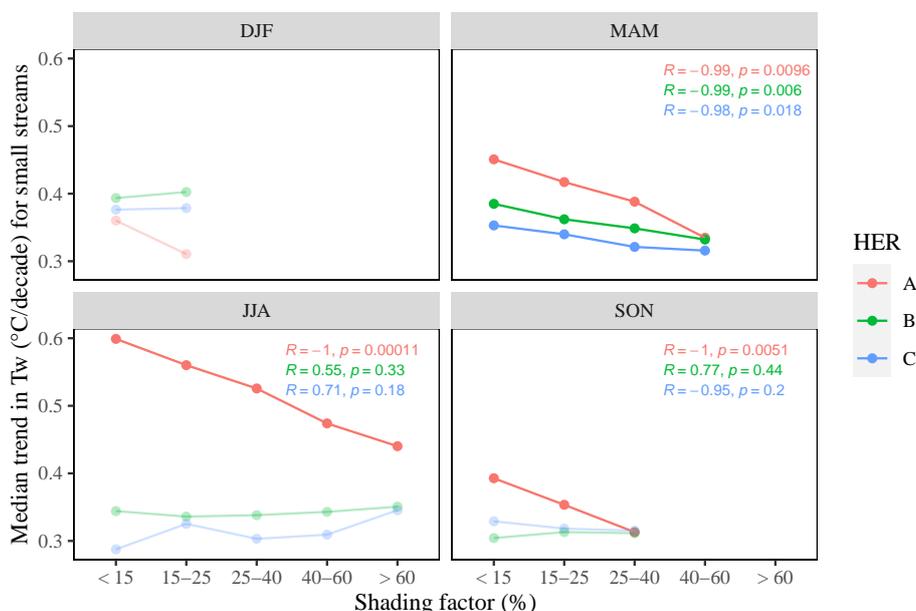


Figure 10. Relationships between shading factor and median trends in Tw over the 1963-2019 period for small streams, by HER and by season. Note that some shading factor classes are not observed in fall and winter. Correlations and associated p-values are shown on the top-right corner of each graph, and significant relationships at the 95 % confidence level are identified by full solid lines.

studies (see e.g. Spinoni et al., 2017; Trambly et al., 2020; Hobeichi et al., 2021). Moreover, Vicente-Serrano et al. (2019) attributed annual streamflow trends in southern France mostly to trends in precipitation and potential evapotranspiration, as opposed to irrigation and land-use changes that have additional strong effects e.g. in the Iberian peninsula. In Switzerland, Michel et al. (2020) described an increase of $+0.33 \pm 0.03^\circ\text{C}/\text{decade}$ in Tw, resulting from the joint effects of increasing in Ta ($+0.39 \pm 0.14^\circ\text{C}/\text{decade}$) and decreasing in Q ($-10.1 \pm 4.6\%/decade$) over the 1979–2018 period. In contrast with our results, they found Tw trends lower than Ta trends due to influence of snow melt and glacier melt. Trends in Tw might also be explained by trends in additional drivers, like shortwave radiation (Wanders et al., 2019), which is the dominant flux at air-water surface, and is notably increasing over Europe (Sanchez-Lorenzo et al., 2015). This might explain discrepancies between Tw and Ta trends in spring and summer, when no decreasing trend in Q are found (see Fig. 3).

Strong synchronicity between Ta and Tw anomalies was observed in the present study in the warmest years, and these years were also among those with the largest negative Q anomalies (see Fig. 8). Indeed, increase in summer Tw could be due to co-occurrence with the increase in summer Ta (average correlation: $+0.82$), and with decrease in summer Q (average correlation: -0.40). These findings are consistent with those of Michel et al. (2020): average Tw-Ta correlation: $+0.61$, and average Tw-Q correlation: -0.66 . For the middle Loire river, Moatar and Gailhard (2006) found that the increase in Ta (resp. decrease in Q) explain 60 % (resp. 40 %) of the increase in Tw. Moreover, the significant change-point in Tw, Ta and Q time series in the late 1980s has also been found in other studies in Europe (Moatar and Gailhard, 2006; Arora et al., 2016; Zobrist et al., 2018; Ptak



et al., 2019b; Michel et al., 2020). Long-term observational time series like that of the Loire at Dampierre also display a similar
350 change-point.

5.4 Natural trends and anthropogenic influence on T_w

Natural T_w time series were used in the current study for detecting trends, as both EROS and T-NET models are used in a non-influenced set-up (see Sect. 3.1). However, anthropogenic impoundments (e.g. large dams, small reservoirs, and ponds) influence downstream T_w regimes in a diversity of ways that depend on their structure and position along the river continuum
355 (Seyedhashemi et al., 2020). In this regard, on the one hand, large dams, by releasing cold hypolimnetic water in summer, can lower downstream T_w (Olden and Naiman, 2010), and mitigate increasing trend in T_w (Cheng et al., 2020). Nevertheless, it is anticipated that a considerable proportion of streams regulated by large reservoirs may still experience high temperatures and low flows under future climate change (Cheng et al., 2020). The mitigating influence of dams could be of importance for streams in the southern headwaters of the Loire basin since this area both experienced the greatest T_w trends and gathers most
360 of existing large dams. On the other hand, ponds and shallow reservoirs, by releasing warm water can increase downstream T_w (Seyedhashemi et al., 2020; Zaidel et al., 2020; Chandesris et al., 2019) and exacerbate increasing trends in T_w (Wanders et al., 2019; Michel et al., 2020). Nevertheless, the warming effect can be local, and unregulated streams being located closer to such regulated streams may show limited to no warming (Wanders et al., 2019). The warming effect of such surface waters in the current study seem more significant for streams located in lowlands in the middle and north of the Loire River basin
365 where most of the shallow reservoirs are located. In these streams, anthropogenically-induced trends in T_w may be greater than natural ones, and the warming process can get worse through the increasing demand for storing water in small reservoirs for irrigation.

5.5 Implications for river management and aquatic biota

The removal of riparian vegetation can increase T_w (Caissie, 2006), and changes in T_w can be even more sensitive to changes
370 in riparian vegetation than to changes in T_a or Q (Wondzell et al., 2019). We showed that in small streams, an increase of > 25 % of riparian shading could decrease the median trend in spring and summer T_w by 5-16 % (Fig. 10). Spring and summer T_w trends were more pronounced in large rivers, especially in the south of the basin, with a difference in median T_w trends of up to +0.18 °C/decade (Fig. 9), probably due to decrease in Q (up to -2 %/decade, see Fig. S12), greater thermal sensitivity, and the absence of mitigating factors like riparian vegetation shading or groundwater inputs (Kelleher et al., 2012; Beaufort
375 et al., 2020).

Restoring riparian vegetation and shading can therefore substantially mitigate future increases in T_w . In addition, riparian restoration may lessen the impacts of climate change on flood damage to human infrastructure, on riparian biodiversity, on ecosystem vulnerability and on changes in Q (Palmer et al., 2009; Seavy et al., 2009; Perry et al., 2015). However, riparian restoration is not an easy task since the survival, persistence, growth rate of planted species as well as required time for thermal
380 regime recovery under possibly severe future conditions should be studied beforehand (Perry et al., 2015). For instance, it may take between 5 and 15 years for rivers to recover their thermal regime following vegetation growth (Caissie, 2006; Edmonds



et al., 2000). Moreover, the efficacy of riparian planting is also highly dependent upon the type and structure of forest stands (Dugdale et al., 2018), and this should also be considered in long-term projects.

Stream warming affects cold-water fish populations negatively at the warmer boundaries of their habitat (Hari et al., 2006).
385 Furthermore, changes in spawning and migration timing (McCann et al., 2018; Arevalo et al., 2020), decreases in habitat availability and freshwater quality for organisms (Lennox et al., 2019), and shifts in species distribution (Comte et al., 2013) are already observed consequences of the long-term increase in T_w . Some major changes in fish density and community structure has already been reported in large rivers over France (Maire et al., 2019) for which we also found greater trends in T_w compared to small ones. Therefore, physical process-based thermal models like T-NET can also be used to assess the various
390 stresses on freshwater habitat sustainability due to changes in Q and T_w (Morales-Marín et al., 2019).

6 Conclusions

Regional trends in T_w at the reach resolution were detected and assessed by using the T-NET physical process-based model coupled with the EROS hydrological model over the Loire basin. Using model outputs across 52 278 reaches over the Loire basin, for 3 variables (T_a , Q , and T_w), and 5 time scales (seasons plus annual), we found consistent increasing T_w trends at
395 the scale of the entire Loire River basin, regardless of the season. Critically, the rate of warming for stream temperature was in the majority of cases higher than the rate of atmospheric warming, suggesting a decoupling of thermal trajectories linked to decreasing Q , especially in the southern headwaters. Moreover, T_w trends in all seasons except winter were greater in rivers with Strahler order > 5 , which we attributed to the mitigation effect of riparian shading for large rivers.

The synchronicity of extreme events of low flows and high air temperature in the southern headwaters will likely generate
400 a double penalty for existing cold-water aquatic communities. However, riparian shading in small mountainous streams may mitigate such warming. These findings underscore that T_a alone is likely not an adequate proxy to explain stresses and shifts experienced by aquatic communities over time and space, especially in regions with more pronounced stream warming, and thus there is a need to grow and maintain T_w sensor networks. This knowledge can help develop appropriate management strategies to conserve thermal refugia and mitigate extreme thermal events induced by climate change.

405 *Author contributions.* HS: Conceptualization, Methodology, Software, Formal analysis, Writing - original draft preparation JPV: Conceptualization, Methodology, Writing - review and editing; JD: Methodology; Writing - review and editing; DT: Resources, Writing - review; CM: Resources; FH: Resources; AM: Writing - review and editing; FM: Conceptualization, Methodology, Writing - review and editing, Supervision

Competing interests. The authors declare that they have no conflict of interest.



- 410 *Acknowledgements.* This work was realized in the course of a doctoral project at University of Tours, funded by European Regional Development Fund (Fonds Européen de développement Régional-FEDER) POI FEDER Loire n°2017- EX001784, Le plan Loire grandeur nature, Agence de l'eau Loire-Bretagne (AELB) and EDF (Hynes Team). The SAFRAN database was provided by the French national meteorological service (Météo-France). Stream temperature data were provided by the Office français de la biodiversité (OFB), Fédération de Pêche (fishing federation). We are grateful to Electricité de France (French Electricity, EDF) for providing long-term data on observed stream
- 415 temperature and naturalized streamflows. We also thank André Chandèsris for his assistance in the incorporation of vegetation cover into the T-NET thermal model.



References

- Allen, R. G., Pereira, L. S., Raes, D., and Smith, M.: Crop Evapotranspiration – Guidelines for computing crop water requirements, FAO Irrigation and Drainage Paper 56, FAO, <http://www.kimberly.uidaho.edu/water/fao56/>, 1998.
- 420 Arevalo, E., Lassalle, G., Tétard, S., Maire, A., Sauquet, E., Lambert, P., Paumier, A., Villeneuve, B., and Drouineau, H.: An innovative bivariate approach to detect joint temporal trends in environmental conditions: Application to large French rivers and diadromous fish, *Science of the Total Environment*, 748, 141 260, <https://doi.org/10.1016/j.scitotenv.2020.141260>, 2020.
- Arismendi, I., Johnson, S. L., Dunham, J. B., Haggerty, R., and Hockman-Wert, D.: The paradox of cooling streams in a warming world: regional climate trends do not parallel variable local trends in stream temperature in the Pacific continental United States, *Geophysical*
425 *Research Letters*, 39, <https://doi.org/10.1029/2012GL051448>, 2012.
- Arismendi, I., Johnson, S. L., Dunham, J. B., and Haggerty, R.: Descriptors of natural thermal regimes in streams and their responsiveness to change in the Pacific Northwest of North America, *Freshwater Biology*, 58, 880–894, <https://doi.org/10.1111/fwb.12094>, 2013a.
- Arismendi, I., Safeeq, M., Johnson, S. L., Dunham, J. B., and Haggerty, R.: Increasing synchrony of high temperature and low flow in western North American streams: double trouble for coldwater biota?, *Hydrobiologia*, 712, 61–70, [https://doi.org/10.1007/s10750-012-](https://doi.org/10.1007/s10750-012-1327-2)
430 [1327-2](https://doi.org/10.1007/s10750-012-1327-2), 2013b.
- Arismendi, I., Safeeq, M., Dunham, J. B., and Johnson, S. L.: Can air temperature be used to project influences of climate change on stream temperature?, *Environmental Research Letters*, 9, 084 015, <https://doi.org/10.1088/1748-9326/9/8/084015>, 2014.
- Arora, R., Tockner, K., and Venohr, M.: Changing river temperatures in northern Germany: trends and drivers of change, *Hydrological Processes*, 30, 3084–3096, <https://doi.org/10.1002/hyp.10849>, 2016.
- 435 Bauer, D. F.: Constructing confidence sets using rank statistics, *Journal of the American Statistical Association*, 67, 687–690, <https://doi.org/10.1080/01621459.1972.10481279>, 1972.
- Beaufort, A., Curie, F., Moatar, F., Ducharme, A., Melin, E., and Thiéry, D.: T-NET, a dynamic model for simulating daily stream temperature at the regional scale based on a network topology, *Hydrological Processes*, 30, 2196–2210, <https://doi.org/10.1002/hyp.10787>, 2016.
- Beaufort, A., Moatar, F., Sauquet, E., Loicq, P., and Hannah, D. M.: Influence of landscape and hydrological factors on stream–air temperature
440 relationships at regional scale, *Hydrological Processes*, 34, 583–597, <https://doi.org/10.1002/hyp.13608>, 2020.
- Benyahya, L., Caissie, D., St-Hilaire, A., Ouarda, T. B., and Bobée, B.: A review of statistical water temperature models, *Canadian Water Resources Journal*, 32, 179–192, <https://doi.org/10.4296/cwrj3203179>, 2007.
- Blöschl, G., Hall, J., Viglione, A., Perdigão, R. A., Parajka, J., Merz, B., Lun, D., Arheimer, B., Aronica, G. T., Bilibashi, A., et al.: Changing climate both increases and decreases European river floods, *Nature*, 573, 108–111, <https://doi.org/10.1038/s41586-019-1495-6>, 2019.
- 445 Bruno, D., Belmar, O., Maire, A., Morel, A., Dumont, B., and Datry, T.: Structural and functional responses of invertebrate communities to climate change and flow regulation in alpine catchments, *Global change biology*, 25, 1612–1628, <https://doi.org/10.1111/gcb.14581>, 2019.
- Buisson, L. and Grenouillet, G.: Contrasted impacts of climate change on stream fish assemblages along an environmental gradient, *Diversity and Distributions*, 15, 613–626, <https://doi.org/10.1111/j.1472-4642.2009.00565.x>, 2009.
- 450 Buisson, L., Blanc, L., and Grenouillet, G.: Modelling stream fish species distribution in a river network: the relative effects of temperature versus physical factors, *Ecology of Freshwater Fish*, 17, 244–257, <https://doi.org/10.1111/j.1600-0633.2007.00276.x>, 2008.



- Bustillo, V., Moatar, F., Ducharne, A., Thiéry, D., and Poirel, A.: A multimodel comparison for assessing water temperatures under changing climate conditions via the equilibrium temperature concept: case study of the Middle Loire River, France, *Hydrological Processes*, 28, 1507–1524, <https://doi.org/10.1002/hyp.9683>, 2014.
- 455 Caissie, D.: The thermal regime of rivers: a review, *Freshwater biology*, 51, 1389–1406, <https://doi.org/10.1111/j.1365-2427.2006.01597.x>, 2006.
- Caissie, D., Satish, M. G., and El-Jabi, N.: Predicting water temperatures using a deterministic model: Application on Miramichi River catchments (New Brunswick, Canada), *Journal of Hydrology*, 336, 303–315, <https://doi.org/10.1016/j.jhydrol.2007.01.008>, 2007.
- Chandesris, A., Van Looy, K., Diamond, J. S., and Souchon, Y.: Small dams alter thermal regimes of downstream water., *Hydrology & Earth*
460 *System Sciences*, 23, <https://doi.org/10.5194/hess-23-4509-2019>, 2019.
- Cheng, Y., Voisin, N., Yearsley, J. R., and Nijssen, B.: Reservoirs modify river thermal regime sensitivity to climate change: a case study in the southeastern United States, *Water Resources Research*, 56, e2019WR025784, <https://doi.org/10.1029/2019WR025784>, 2020.
- Comte, L., Buisson, L., Daufresne, M., and Grenouillet, G.: Climate-induced changes in the distribution of freshwater fish: observed and predicted trends, *Freshwater Biology*, 58, 625–639, <https://doi.org/10.1111/fwb.12081>, 2013.
- 465 Dan Moore, R., Spittlehouse, D., and Story, A.: Riparian microclimate and stream temperature response to forest harvesting: A review, *JAWRA Journal of the American Water Resources Association*, 41, 813–834, <https://doi.org/10.1111/j.1752-1688.2005.tb03772.x>, 2005.
- Domisch, S., Araújo, M. B., Bonada, N., Pauls, S. U., Jähnig, S. C., and Haase, P.: Modelling distribution in European stream macroinvertebrates under future climates, *Global Change Biology*, 19, 752–762, <https://doi.org/10.1111/gcb.12107>, 2013.
- Ducharne, A.: Importance of stream temperature to climate change impact on water quality, *Hydrology and Earth System Sciences*,
470 <https://doi.org/10.5194/hess-12-797-2008>, 2008.
- Dugdale, S. J., Hannah, D. M., and Malcolm, I. A.: River temperature modelling: A review of process-based approaches and future directions, *Earth-Science Reviews*, 175, 97–113, <https://doi.org/10.1016/j.earscirev.2017.10.009>, 2017.
- Dugdale, S. J., Malcolm, I. A., Kantola, K., and Hannah, D. M.: Stream temperature under contrasting riparian forest cover: Understanding thermal dynamics and heat exchange processes, *Science of The Total Environment*, 610, 1375–1389,
475 <https://doi.org/10.1016/j.scitotenv.2017.08.198>, 2018.
- Edmonds, R., Murray, G., and Marra, J.: Influence of partial harvesting on stream temperatures, chemistry, and turbidity in forests on the western Olympic Peninsula, Washington, WSU Press, <http://hdl.handle.net/2376/1065>, 2000.
- Floury, M., Usseglio-Polatera, P., Ferreol, M., Delattre, C., and Souchon, Y.: Global climate change in large European rivers: long-term effects on macroinvertebrate communities and potential local confounding factors, *Global change biology*, 19, 1085–1099,
480 <https://doi.org/10.1111/gcb.12124>, 2013.
- Giuntoli, I., Renard, B., Vidal, J.-P., and Bard, A.: Low flows in France and their relationship to large-scale climate indices, *Journal of Hydrology*, 482, 105–118, <https://doi.org/10.1016/j.jhydrol.2012.12.038>, 2013.
- Hannah, D. M. and Garner, G.: River water temperature in the United Kingdom: changes over the 20th century and possible changes over the 21st century, *Progress in Physical Geography*, 39, 68–92, <https://doi.org/10.1177/2F0309133314550669>, 2015.
- 485 Hannah, D. M., Malcolm, I. A., Soulsby, C., and Youngson, A. F.: Heat exchanges and temperatures within a salmon spawning stream in the Cairngorms, Scotland: seasonal and sub-seasonal dynamics, *River Research and Applications*, 20, 635–652, <https://doi.org/10.1002/tra.771>, 2004.



- Hari, R. E., Livingstone, D. M., Siber, R., BURKHARDT-HOLM, P., and Guettinger, H.: Consequences of climatic change for water temperature and brown trout populations in Alpine rivers and streams, *Global Change Biology*, 12, 10–26, <https://doi.org/10.1111/j.1365-2486.2005.001051.x>, 2006.
- Hobeichi, S., Abramowitz, G., and Evans, J. P.: Robust historical evapotranspiration trends across climate regimes, *Hydrology and Earth System Sciences*, 25, 3855–3874, <https://doi.org/10.5194/hess-25-3855-2021>, 2021.
- Huntington, T. G.: Evidence for intensification of the global water cycle: review and synthesis, *Journal of Hydrology*, 319, 83–95, <https://doi.org/10.1016/j.jhydrol.2005.07.003>, 2006.
- 495 Hutchison, B. A. and Matt, D. R.: The distribution of solar radiation within a deciduous forest, *Ecological Monographs*, 47, 185–207, <https://doi.org/10.2307/1942616>, 1977.
- IGN: Descriptif technique BD TOPO, Tech. rep., Institut Gógraphique National, https://www.cc-saulnois.fr/sig/documents/BDTOPO/DC_BDTOPO_2.pdf, 2008.
- IGN: Descriptif technique BD ALTI, Tech. rep., Institut Gógraphique National, [https://geoservices.ign.fr/ressources_documentaires/Espace_](https://geoservices.ign.fr/ressources_documentaires/Espace_documentaire/MODELES_3D/BDALTI2/DC_BDALTI_2-0.pdf)
- 500 [documentaire/MODELES_3D/BDALTI2/DC_BDALTI_2-0.pdf](https://geoservices.ign.fr/ressources_documentaires/Espace_documentaire/MODELES_3D/BDALTI2/DC_BDALTI_2-0.pdf), 2011.
- Isaak, D., Wollrab, S., Horan, D., and Chandler, G.: Climate change effects on stream and river temperatures across the northwest US from 1980–2009 and implications for salmonid fishes, *Climatic change*, 113, 499–524, <https://doi.org/10.1007/s10584-011-0326-z>, 2012.
- Isaak, D. J., Wenger, S. J., Peterson, E. E., Ver Hoef, J. M., Nagel, D. E., Luce, C. H., Hostetler, S. W., Dunham, J. B., Roper, B. B., Wollrab, S. P., et al.: The NorWeST summer stream temperature model and scenarios for the western US: A crowd-sourced database and new geospatial tools foster a user community and predict broad climate warming of rivers and streams, *Water Resources Research*, 53, 9181–9205, <https://doi.org/10.1002/2017WR020969>, 2017.
- 505 Jackson, F., Hannah, D. M., Fryer, R., Millar, C., and Malcolm, I.: Development of spatial regression models for predicting summer river temperatures from landscape characteristics: Implications for land and fisheries management, *Hydrological processes*, 31, 1225–1238, <https://doi.org/10.1002/hyp.11087>, 2017.
- 510 Jackson, F. L., Fryer, R. J., Hannah, D. M., Millar, C. P., and Malcolm, I. A.: A spatio-temporal statistical model of maximum daily river temperatures to inform the management of Scotland’s Atlantic salmon rivers under climate change, *Science of the Total Environment*, 612, 1543–1558, <https://doi.org/10.1016/j.scitotenv.2017.09.010>, 2018.
- Johnson, S. L.: Factors influencing stream temperatures in small streams: substrate effects and a shading experiment, *Canadian Journal of Fisheries and Aquatic Sciences*, 61, 913–923, <https://doi.org/10.1139/f04-040>, 2004.
- 515 Kaushal, S. S., Likens, G. E., Jaworski, N. A., Pace, M. L., Sides, A. M., Seekell, D., Belt, K. T., Secor, D. H., and Wingate, R. L.: Rising stream and river temperatures in the United States, *Frontiers in Ecology and the Environment*, 8, 461–466, <https://doi.org/10.1890/090037>, 2010.
- Kędra, M.: Regional response to global warming: Water temperature trends in semi-natural mountain river systems, *Water*, 12, 283, <https://doi.org/10.3390/w12010283>, 2020.
- 520 Kelleher, C., Wagener, T., Gooseff, M., McGlynn, B., McGuire, K., and Marshall, L.: Investigating controls on the thermal sensitivity of Pennsylvania streams, *Hydrological Processes*, 26, 771–785, <https://doi.org/10.1002/hyp.8186>, 2012.
- Kurylyk, B. L., Bourque, C.-A., and MacQuarrie, K. T.: Potential surface temperature and shallow groundwater temperature response to climate change: an example from a small forested catchment in east-central New Brunswick (Canada), *Hydrology and Earth System Sciences*, 17, 2701–2716, <https://doi.org/10.5194/hess-17-2701-2013>, 2013.



- 525 Kurylyk, B. L., MacQuarrie, K. T., and Voss, C. I.: Climate change impacts on the temperature and magnitude of groundwater discharge from shallow, unconfined aquifers, *Water Resources Research*, 50, 3253–3274, <https://doi.org/10.1002/2013WR014588>, 2014.
- Lennox, R. J., Crook, D. A., Moyle, P. B., Struthers, D. P., and Cooke, S. J.: Toward a better understanding of freshwater fish responses to an increasingly drought-stricken world, *Reviews in fish biology and fisheries*, 29, 71–92, <https://doi.org/10.1007/s11160-018-09545-9>, 2019.
- Li, G., Jackson, C. R., and Krasieski, K. A.: Modeled riparian stream shading: Agreement with field measurements and sensitivity to riparian conditions, *Journal of hydrology*, 428, 142–151, <https://doi.org/10.1016/j.jhydrol.2012.01.032>, 2012.
- 530 Loicq, P., Moatar, F., Jullian, Y., Dugdale, S. J., and Hannah, D. M.: Improving representation of riparian vegetation shading in a regional stream temperature model using LiDAR data, *Science of the total environment*, 624, 480–490, <https://doi.org/10.1016/j.scitotenv.2017.12.129>, 2018.
- Maire, A., Thierry, E., Viechtbauer, W., and Daufresne, M.: Poleward shift in large-river fish communities detected with a novel meta-analysis framework, *Freshwater Biology*, 64, 1143–1156, <https://doi.org/10.1111/fwb.13291>, 2019.
- 535 Majdi, N., Uthoff, J., Traunspurger, W., Laffaille, P., and Maire, A.: Effect of water warming on the structure of biofilm-dwelling communities, *Ecological Indicators*, 117, 106 622, <https://doi.org/10.1016/j.ecolind.2020.106622>, 2020.
- Mann, H. B.: Nonparametric tests against trend, *Econometrica: Journal of the econometric society*, pp. 245–259, <https://doi.org/10.2307/1907187>, 1945.
- 540 Mantua, N., Tohver, I., and Hamlet, A.: Climate change impacts on streamflow extremes and summertime stream temperature and their possible consequences for freshwater salmon habitat in Washington State, *Climatic Change*, 102, 187–223, <https://doi.org/10.1007/s10584-010-9845-2>, 2010.
- Mayer, T. D.: Controls of summer stream temperature in the Pacific Northwest, *Journal of Hydrology*, 475, 323–335, <https://doi.org/10.1016/j.jhydrol.2012.10.012>, 2012.
- 545 McCann, E. L., Johnson, N. S., and Pangle, K. L.: Corresponding long-term shifts in stream temperature and invasive fish migration, *Canadian Journal of Fisheries and Aquatic Sciences*, 75, 772–778, <https://doi.org/10.1139/cjfas-2017-0195>, 2018.
- Meisner, J. D.: Potential loss of thermal habitat for brook trout, due to climatic warming, in two southern Ontario streams, *Transactions of the American Fisheries Society*, 119, 282–291, [https://doi.org/10.1577/1548-8659\(1990\)119%3C0282:PLOTHF%3E2.3.CO;2](https://doi.org/10.1577/1548-8659(1990)119%3C0282:PLOTHF%3E2.3.CO;2), 1990.
- Michel, A., Brauchli, T., Lehning, M., Schaepli, B., and Huwald, H.: Stream temperature and discharge evolution in Switzerland over the last 50 years: annual and seasonal behaviour., *Hydrology & Earth System Sciences*, 24, <https://doi.org/10.5194/hess-24-115-2020>, 2020.
- 550 Moatar, F. and Dupont, N.: La Loire fluviale et estuarienne: un milieu en évolution, Editions Quae, <https://www.quae.com/produit/1334/9782759224036/la-loire-fluviale-et-estuarienne>, 2016.
- Moatar, F. and Gailhard, J.: Water temperature behaviour in the River Loire since 1976 and 1881, *Comptes Rendus Geoscience*, 338, 319–328, <https://doi.org/10.1016/j.crte.2006.02.011>, 2006.
- 555 Mohseni, O., Erickson, T. R., and Stefan, H. G.: Sensitivity of stream temperatures in the United States to air temperatures projected under a global warming scenario, *Water Resources Research*, 35, 3723–3733, <https://doi.org/10.1029/1999WR900193>, 1999.
- Morales-Marín, L., Rokaya, P., Sanyal, P., Sereda, J., and Lindenschmidt, K.: Changes in streamflow and water temperature affect fish habitat in the Athabasca River basin in the context of climate change, *Ecological Modelling*, 407, 108 718, <https://doi.org/10.1016/j.ecolmodel.2019.108718>, 2019.
- 560 Morel, M., Booker, D. J., Gob, F., and Lamouroux, N.: Intercontinental predictions of river hydraulic geometry from catchment physical characteristics, *Journal of Hydrology*, 582, 124 292, <https://doi.org/10.1016/j.jhydrol.2019.124292>, 2020.



- Nash, J. E. and Sutcliffe, J. V.: River Flow Forecasting Through Conceptual Models. Part 1: A Discussion of Principles, *Journal of Hydrology*, 10, 282–290, [https://doi.org/10.1016/0022-1694\(70\)90255-6](https://doi.org/10.1016/0022-1694(70)90255-6), 1970.
- Nelson, K. C. and Palmer, M. A.: Stream temperature surges under urbanization and climate change: data, models, and responses 1, *JAWRA Journal of the American Water Resources Association*, 43, 440–452, <https://doi.org/10.1111/j.1752-1688.2007.00034.x>, 2007.
- 565 Niedrist, G. H. and Füreder, L.: Real-time warming of alpine streams:(Re) defining invertebrates' temperature preferences, *River Research and Applications*, 37, 283–293, <https://doi.org/10.1002/rra.3638>, 2021.
- O'Gorman, E. J., Pichler, D. E., Adams, G., Benstead, J. P., Cohen, H., Craig, N., Cross, W. F., Demars, B. O., Friberg, N., Gislason, G. M., et al.: Impacts of warming on the structure and functioning of aquatic communities: individual-to ecosystem-level responses, *Advances in*
- 570 *ecological research*, 47, 81–176, <https://doi.org/10.1016/B978-0-12-398315-2.00002-8>, 2012.
- Olden, J. D. and Naiman, R. J.: Incorporating thermal regimes into environmental flows assessments: modifying dam operations to restore freshwater ecosystem integrity, *Freshwater Biology*, 55, 86–107, <https://doi.org/10.1111/j.1365-2427.2009.02179.x>, 2010.
- Orr, H. G., Simpson, G. L., des Clers, S., Watts, G., Hughes, M., Hannaford, J., Dunbar, M. J., Laizé, C. L., Wilby, R. L., Battarbee, R. W., et al.: Detecting changing river temperatures in England and Wales, *Hydrological Processes*, 29, 752–766,
- 575 <https://doi.org/10.1002/hyp.10181>, 2015.
- Palmer, M. A., Lettenmaier, D. P., Poff, N. L., Postel, S. L., Richter, B., and Warner, R.: Climate change and river ecosystems: protection and adaptation options, *Environmental management*, 44, 1053–1068, <https://doi.org/10.1007/s00267-009-9329-1>, 2009.
- Pella, H., Lejot, J., Lamouroux, N., and Snelder, T.: Le réseau hydrographique théorique (RHT) français et ses attributs environnementaux, *Géomorphologie: relief, processus, environnement*, 18, 317–336, <https://doi.org/10.4000/geomorphologie.9933>, 2012.
- 580 Perry, L. G., Reynolds, L. V., Beechie, T. J., Collins, M. J., and Shafroth, P. B.: Incorporating climate change projections into riparian restoration planning and design, *Ecohydrology*, 8, 863–879, <https://doi.org/10.1002/eco.1645>, 2015.
- Pettitt, A. N.: A non-parametric approach to the change-point problem, *Applied Statistics*, 28, 126–135, <https://doi.org/10.2307/2346729>, 1979.
- Poole, G. C. and Berman, C. H.: An ecological perspective on in-stream temperature: natural heat dynamics and mechanisms of human-
- 585 *caused thermal degradation*, *Environmental management*, 27, 787–802, <https://doi.org/10.1007/s002670010188>, 2001.
- Prudhomme, C., Giuntoli, I., Robinson, E. L., Clark, D. B., Arnell, N. W., Dankers, R., Fekete, B. M., Franssen, W., Gerten, D., Gosling, S. N., et al.: Hydrological droughts in the 21st century, hotspots and uncertainties from a global multimodel ensemble experiment, *Proceedings of the National Academy of Sciences*, 111, 3262–3267, <https://doi.org/10.1073/pnas.1222473110>, 2014.
- Ptak, M., Choiński, A., and Kirviel, J.: Long-term water temperature fluctuations in coastal rivers (southern Baltic) in Poland, *Bulletin of*
- 590 *Geography. Physical Geography Series*, 11, 35–42, <https://doi.org/10.1515/bgeo-2016-0013>, 2016.
- Ptak, M., Sojka, M., Kałuża, T., Choiński, A., and Nowak, B.: Long-term water temperature trends of the Warta River in the years 1960–2009, *Ecohydrology & Hydrobiology*, 19, 441–451, <https://doi.org/10.1016/j.ecohyd.2019.03.007>, 2019a.
- Ptak, M., Sojka, M., and Kozłowski, M.: The increasing of maximum lake water temperature in lowland lakes of Central Europe: case study of the Polish Lakeland, in: *Annales de Limnologie-International Journal of Limnology*, vol. 55, p. 6, EDP Sciences,
- 595 <https://doi.org/10.1051/limn/2019005>, 2019b.
- Quintana-Segui, P., Le Moigne, P., Durand, Y., Martin, E., Habets, F., Baillon, M., Canellas, C., Franchisteguy, L., and Morel, S.: Analysis of near-surface atmospheric variables: Validation of the SAFRAN analysis over France, *Journal of applied meteorology and climatology*, 47, 92–107, <https://doi.org/10.1175/2007JAMC1636.1>, 2008.



- Romaní, A. M., Boulètreau, S., Villanueva, V. D., Garabetian, F., Marxsen, J., Norf, H., Pohlen, E., Weitere, M., et al.: Microbes in aquatic
600 biofilms under the effect of changing climate., *Climate change and microbial ecology: Current research and future trends*, pp. 83–96,
2016.
- Sanchez-Lorenzo, A., Wild, M., Brunetti, M., Guijarro, J. A., Hakuba, M. Z., Calbó, J., Mystakidis, S., and Bartok, B.: Reassessment
and update of long-term trends in downward surface shortwave radiation over Europe (1939–2012), *Journal of Geophysical Research:*
Atmospheres, 120, 9555–9569, <https://doi.org/10.1002/2015JD023321>, 2015.
- 605 Scheffers, B. R., De Meester, L., Bridge, T. C., Hoffmann, A. A., Pandolfi, J. M., Corlett, R. T., Butchart, S. H., Pearce-Kelly,
P., Kovacs, K. M., Dudgeon, D., et al.: The broad footprint of climate change from genes to biomes to people, *Science*, 354,
<https://doi.org/10.1126/science.aaf7671>, 2016.
- Seavy, N. E., Gardali, T., Golet, G. H., Griggs, F. T., Howell, C. A., Kelsey, R., Small, S. L., Viers, J. H., and Weigand, J. F.: Why climate
change makes riparian restoration more important than ever: recommendations for practice and research, *Ecological Restoration*, 27,
610 330–338, <https://doi.org/10.3368/er.27.3.330>, 2009.
- Sen, P. K.: Estimates of the regression coefficient based on Kendall's tau, *Journal of the American statistical association*, 63, 1379–1389,
<https://doi.org/10.1080/01621459.1968.10480934>, 1968.
- Seyedhashemi, H., Moatar, F., Vidal, J.-P., Diamond, J. S., Beaufort, A., Chandesris, A., and Valette, L.: Thermal signatures iden-
tify the influence of dams and ponds on stream temperature at the regional scale, *Science of The Total Environment*, p. 142667,
615 <https://doi.org/10.1016/j.scitotenv.2020.142667>, 2020.
- Sinokrot, B., Stefan, H., McCormick, J., and Eaton, J.: Modeling of climate change effects on stream temperatures and fish habitats below
dams and near groundwater inputs, *Climatic Change*, 30, 181–200, <https://doi.org/10.1007/BF01091841>, 1995.
- Spinoni, J., Naumann, G., and Vogt, J. V.: Pan-European seasonal trends and recent changes of drought frequency and severity, *Global and
Planetary Change*, 148, 113–130, <https://doi.org/10.1016/j.gloplacha.2016.11.013>, 2017.
- 620 Stefan, H. G. and Preud'homme, E. B.: Stream temperature estimation from air temperature 1, *JAWRA Journal of the American Water
Resources Association*, 29, 27–45, <https://doi.org/10.1111/j.1752-1688.1993.tb01502.x>, 1993.
- Stefani, F., Schiavon, A., Tirozzi, P., Gomarasca, S., and Marziali, L.: Functional response of fish communities in a multistressed freshwater
world, *Science of The Total Environment*, 740, 139 902, <https://doi.org/10.1016/j.scitotenv.2020.139902>, 2020.
- Taylor, C. A. and Stefan, H. G.: Shallow groundwater temperature response to climate change and urbanization, *Journal of Hydrology*, 375,
625 601–612, <https://doi.org/10.1016/j.jhydrol.2009.07.009>, 2009.
- Thiéry, D.: Forecast of changes in piezometric levels by a lumped hydrological model, *Journal of Hydrology*, 97, 129–148,
[https://doi.org/10.1016/0022-1694\(88\)90070-4](https://doi.org/10.1016/0022-1694(88)90070-4), 1988.
- Thiéry, D.: Logiciel ÉROS version 7.1–Guide d'utilisation, Rapport final, Tech. rep., BRGM/RP-67704-FR, BRGM, Orléans, [http://infoterre.
brgm.fr/rapports/RP-67704-FR.pdf](http://infoterre.brgm.fr/rapports/RP-67704-FR.pdf), 2018.
- 630 Thiéry, D. and Moutzopoulos, C.: Un modèle hydrologique spatialisé pour la simulation de très grands bassins: le modèle EROS formé de
grappes de modèles globaux élémentaires, VIIIèmes journées hydrologiques de l'ORSTOM" Régionalisation en hydrologie, application
au développement", Le Barbé et E. Servat (Eds.), pp. 285–295, <https://hal-brgm.archives-ouvertes.fr/hal-01061971>, 1995.
- Tisseuil, C., Vrac, M., Grenouillet, G., Wade, A. J., Gevrey, M., Oberdorff, T., Grodwohl, J.-B., and Lek, S.: Strengthening the link between
climate, hydrological and species distribution modeling to assess the impacts of climate change on freshwater biodiversity, *Science of the
635 total environment*, 424, 193–201, <https://doi.org/10.1016/j.scitotenv.2012.02.035>, 2012.



- Tramblay, Y., Koutroulis, A., Samaniego, L., Vicente-Serrano, S. M., Volaire, F., Boone, A., Le Page, M., Llasat, M. C., Albergel, C., Burak, S., Cailleret, M., Cindrić Kalin, K., Davi, H., Dupuy, J.-L., Greve, P., Grillakis, M., Hanich, L., Jarlan, L., Martin-StPaul, N., Martínez-Vilalta, J., Mouillot, F., Pulido-Velazquez, D., Quintana-Seguí, P., Renard, D., Turco, M., Türkeş, M., Trigo, R., Vidal, J.-P., Vilagrosa, A., Zribi, M., and Polcher, J.: Challenges for drought assessment in the Mediterranean region under future climate scenarios, *Earth-Science Reviews*, 210, 103–348, <https://doi.org/10.1016/j.earscirev.2020.103348>, 2020.
- 640 Valette, L., Piffady, J., Chandesris, A., and Souchon, Y.: SYRAH-CE: description des données et modélisation du risque d'altération hydromorphologique des cours d'eau pour l'état des lieux DCE, Rapport Technique Onema-Irstea, http://oai.afbiodiversite.fr/cindocoai/download/PUBLI/1185/1/2012_108.pdf_4080Ko, 2012.
- van Looy, K. and Tormos, T.: Indicateurs spatialisés du fonctionnement des corridors rivulaires, Tech. rep., Irstea, <https://hal.inrae.fr/hal-02599341>, 2013.
- 645 Van Vliet, M., Ludwig, F., Zwolsman, J., Weedon, G., and Kabat, P.: Global river temperatures and sensitivity to atmospheric warming and changes in river flow, *Water Resources Research*, 47, <https://doi.org/10.1029/2010WR009198>, 2011.
- van Vliet, M. T., Franssen, W. H., Yearsley, J. R., Ludwig, F., Haddeland, I., Lettenmaier, D. P., and Kabat, P.: Global river discharge and water temperature under climate change, *Global Environmental Change*, 23, 450–464, <https://doi.org/10.1016/j.gloenvcha.2012.11.002>, 650 2013.
- Vicente-Serrano, S., Hannaford, J., Murphy, C., Peña Gallardo, M., Lorenzo-Lacruz, J., Domínguez-Castro, F., López Moreno, J. I., Beguería, S., Noguear, I., Harrigan, S., and Vidal, J.-P.: Climate, irrigation, and land-cover change explain streamflow trends in countries bordering the Northeast Atlantic, *Geophysical Research Letters*, 46, 10 821–10 833, <https://doi.org/10.1029/2019GL084084>, 2019.
- Vidal, J.-P., Martin, E., Franchistéguy, L., Baillon, M., and Soubeyroux, J.-M.: A 50-year high-resolution atmospheric reanalysis over France 655 with the Safran system, *International Journal of Climatology*, 30, 1627–1644, <https://doi.org/10.1002/joc.2003>, 2010.
- Wanders, N., van Vliet, M. T., Wada, Y., Bierkens, M. F., and van Beek, L. P.: High-resolution global water temperature modeling, *Water Resources Research*, 55, 2760–2778, <https://doi.org/10.1029/2018WR023250>, 2019.
- Wasson, J.-G., Chandesris, A., Pella, H., and Blanc, L.: Typology and reference conditions for surface water bodies in France: the hydroecoregion approach, *TemaNord*, 566, 37–41, <https://hal.archives-ouvertes.fr/hal-00475620/document>, 2002.
- 660 Webb, B.: Trends in stream and river temperature, *Hydrological processes*, 10, 205–226, [https://doi.org/10.1002/\(SICI\)1099-1085\(199602\)10:2<205::AID-HYP358>3.0.CO;2-1](https://doi.org/10.1002/(SICI)1099-1085(199602)10:2<205::AID-HYP358>3.0.CO;2-1), 1996.
- Webb, B. and Walling, D.: Long-term variability in the thermal impact of river impoundment and regulation, *Applied Geography*, 16, 211–223, [https://doi.org/10.1016/0143-6228\(96\)00007-0](https://doi.org/10.1016/0143-6228(96)00007-0), 1996.
- Webb, B. and Walling, D.: Complex summer water temperature behaviour below a UK regulating reservoir, *Regulated Rivers: Research & Management: An International Journal Devoted to River Research and Management*, 13, 463–477, [https://doi.org/10.1002/\(SICI\)1099-1646\(199709/10\)13:5<463::AID-RRR470>3.0.CO;2-1](https://doi.org/10.1002/(SICI)1099-1646(199709/10)13:5<463::AID-RRR470>3.0.CO;2-1), 1997.
- 665 Webb, B. W., Hannah, D. M., Moore, D. R., Brown, L. E., and Nobilis, F.: Recent advances in stream and river temperature research, *Hydrological Processes: An International Journal*, 22, 902–918, <https://doi.org/10.1002/hyp.6994>, 2008.
- Wilby, R. and Johnson, M.: Climate variability and implications for keeping rivers cool in England, *Climate Risk Management*, 30, 100–259, 670 <https://doi.org/10.1016/j.crm.2020.100259>, 2020.
- Wondzell, S. M., Diabat, M., and Haggerty, R.: What matters most: are future stream temperatures more sensitive to changing air temperatures, discharge, or riparian vegetation?, *JAWRA Journal of the American Water Resources Association*, 55, 116–132, <https://doi.org/10.1111/1752-1688.12707>, 2019.



- Woodward, G., Perkins, D. M., and Brown, L. E.: Climate change and freshwater ecosystems: impacts across multiple levels of organization, Philosophical Transactions of the Royal Society B: Biological Sciences, 365, 2093–2106, <https://doi.org/10.1098/rstb.2010.0055>, 2010.
- 675 Yearsley, J. R.: A semi-Lagrangian water temperature model for advection-dominated river systems, Water Resources Research, 45, <https://doi.org/10.1029/2008WR007629>, 2009.
- Zaidel, P. A., Roy, A. H., Houle, K. M., Lambert, B., Letcher, B. H., Nislow, K. H., and Smith, C.: Impacts of small dams on stream temperature, Ecological Indicators, 120, 106 878, <https://doi.org/10.1016/j.ecolind.2020.106878>, 2020.
- 680 Zhu, S., Bonacci, O., Oskoruš, D., Hadzima-Nyarko, M., and Wu, S.: Long term variations of river temperature and the influence of air temperature and river discharge: case study of Kupa River watershed in Croatia, Journal of Hydrology and Hydromechanics, 67, 305–313, <https://doi.org/10.2478/johh-2019-0019>, 2019.
- Zobrist, J., Schoenenberger, U., Figura, S., and Hug, S. J.: Long-term trends in Swiss rivers sampled continuously over 39 years reflect changes in geochemical processes and pollution, Environmental Science and Pollution Research, 25, 16 788–16 809, 685 <https://doi.org/10.1007/s11356-018-1679-x>, 2018.